NEWTONIAN STATIC AND DYNAMIC AERODYNAMIC COEFFICIENTS FOR AN ASYMMETRIC BODY IN PLANAR MOTION

by
D. A. Coulter
W. B. Brooks
J. M. Calligeros

June, 1965

AEROELASTIC AND STRUCTURES RESEARCH LABORATORY
DEPARTMENT OF AERONAUTICS AND ASTRONAUTICS
MASSACHUSETTS INSTITUTE OF TECHNOLOGY
Cambridge, Massachusetts 02139

FOREWORD

D D C

SEP 7 1965

DDC-IRA E
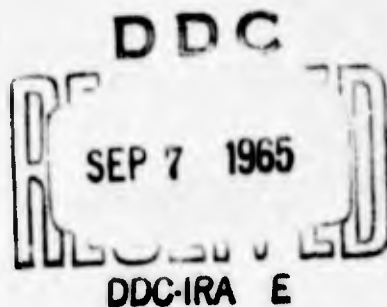
ABSTRACT

The governing equations and a computer program are
developed which calculate the static and dynamic aerodynamic
coefficients for bodies composed of right circular cone frusta.
The resulting combined body possesses one plane of symmetry
and the coefficients are referred to that plane. The center
of gravity and the moment reference point are arbitrary locations
in the plane of symmetry. Flow shielding for the complete
angle of attack range is considered for each frustum segment,
but mutual shielding of one segment on another is neglected.
The effect of any gap-overlap region at the junctions of ro-
tated segments is also neglected.

Example calculations are presented for an asymmetric
conical body and an asymmetric cone-cylinder-flare configuration.

ii

TABLE OF CONTENTS

iv

LIST OF ILLUSTRATIONS

LIST OF PRINCIPAL SYMBOLS

A,B,C...   shape coefficients defined in Eqs. 2.36

C_X axial force coefficient, $X / \frac{1}{2} \rho V_\infty^2 S$

C_N normal force coefficient, $N / \frac{1}{2} \rho V_\infty^2 S$

C_M static pitching moment coefficient, $(M)_{q=0} / \frac{1}{2} \rho V_\infty^2 S d$

C_{Mq} pitch-damping coefficient, $\dfrac{\partial \left(M / \frac{1}{2} \rho V_\infty^2 S d \right)}{\partial \left(q d / 2 V_\infty \right)}$

d   arbitrary reference diameter

$\bar{F}$ resultant force vector

f(x)   surface function defined in Eq. 2.7

$\bar{i}, \bar{j}, \bar{k}$ unit vectors

L   arbitrary reference length

$\bar{l}_{cg}$ vector length from center of gravity to area dS

$\bar{l}_o$ vector length from point x_o, y_o, z_o to area dS

M   total pitching moment about axis through (x_o, z_o), positive nose up

N   normal force, positive up

$\bar{n}$ unit normal surface vector, positive inward

q   angular velocity about axis through (x_{cg}, z_{cg}), positive clockwise

r, θ polar coordinates of body cross-section

S   arbitrary reference area

U local flow velocity

V_∞ free stream velocity

X   axial force, positive rearward

x,y,z,   Cartesian coordinates

α angle of attack

β angle between body segment axis and principal body axis, positive counterclockwise rotation

δ conical frustum angle

Θu integration limit on shielding boundary

$\Phi, \bar{\Phi}_z, \bar{\Phi}_z, \bar{\Phi}_y$ functions defined in Eqs. 2.37

$( )_n, ( )^{(n)}$ referring to n^{th} frustum segment

viii

SECTION I

INTRODUCTION

In many trajectory problems it is necessary to be able to estimate the aerodynamic coefficients for sizable angles of attack. For hypersonic flow, the only alternative to experimental testing that appears tractable at this time is Newtonian impact theory.

As a result of the adaptability of Newtonian theory to conditions involving large angles of attack, many investigations have been carried out heretofore. References 1, 2, 3, for example, consider bodies of revolution under a variety of conditions. Calculations for a body of revolution with an off-set center of gravity are reported in Reference 1 and reasonable correlation with experimental values has been found over the full angle of attack range. Reference 2 treated incomplete bodies of revolution, but at present no attempts seem to have been made to consider small degrees of body asymmetry.

In this report, a computer program has been written to calculate the force, moment, and damping coefficients over the full 360° range of angle of attack for a certain class of bodies. These bodies have one plane of symmetry and are composed of simple conical frusta. Such composite bodies were considered in Ref. 3. However, those results are limited to axisymmetric bodies at zero angle of attack. The static aerodynamic character-istics of a canted cone were considered in Refs. 4 and 5 for small and large angles of attack. The present report, however, is more general in that it considers the pitch-damping-characteristics and is applicable to a body composed of several segments.

---

* Manuscript released by the authors in February 1965.

In computing the overall coefficients in this report, it is assumed that the aerodynamic behavior of the component frusta are independent of any surrounding frusta. This procedure is only approximate since apparently some flow interference will be present for some angle of attack range. Also, an unrealistic gap-overlap region occurs at the junction of segments rotated with respect to each other. For the case of small asymmetries, these effects may be neglected.

In theory, any number of body segments may be taken into account, thus allowing considerable flexibility in the body shapes considered.

SECTION II

ANALYSIS

2.1 General

The basic assumption involved in Newtonian flow theory is that a stream of air impinging upon a surface loses its component of momentum normal to the surface but travels along the surface with its tangential component of momentum unchanged. The force which results is directed inward to the body and is equal to the time rate of change of the normal component of momentum lost by the flow.

Consider a general body, as in Fig. 1, where x, y, z are body axes located at the nose. If $\bar{n}$ is an inwardly directed unit normal vector to an element of area, dS, located at (x, y, z), the inward incremental force on this area, according to Newtonian flow, is

$$\delta \bar{F} = \rho (\bar{U} \cdot \bar{n})^2 dS \, \bar{n} \qquad (2.1)$$

where $\bar{U}$ is the local flow velocity. The moment $\delta \bar{G}$ about an arbitrary point (x_0, y_0, z_0) resulting from this incremental force is

$$\delta \bar{G} = \bar{l}_0 \times \delta \bar{F} \qquad (2.2)$$

where $\bar{l}_0$ is the length vector from (x_0, y_0, z_0) to the area, dS.

A body which is rotating with an angular velocity vector

3

$\bar{\omega}$ and which is immersed in a flow with a free stream velocity $\bar{V}_\infty$, will experience the following relative flow velocity at the point (x,y,z)

$$\bar{U} = \bar{V}_\infty - \bar{\omega} \times \bar{l}_{cg} \qquad (2.3)$$

where $\bar{\omega}$ is the angular velocity vector of a body axis system which is located at the center of gravity and $\bar{l}_{cg}$ is the length vector from the center of gravity to the area dS.

Restricting the motion of the body to the x-z plane, the scalar components of the total force $\bar{F}$ and total moment $\bar{G}$ acting on the body are found from Eqs. 2.1 and 2.2 by integrating over the surface area of the body which is exposed to the flow. The forces X (axial), N (normal) and the moment M about an axis through (x_0, z_0), defined positive as shown in Fig. 2, are

$$X = \rho \int_S (\bar{U} \cdot \bar{n})^2 (\bar{i} \cdot \bar{n}) dS \qquad (2.4)$$

$$N = \rho \int_S (\bar{U} \cdot \bar{n})^2 (\bar{k} \cdot \bar{n}) dS \qquad (2.5)$$

4

$$M = \rho \int_S (\bar{U} \cdot \bar{n})^2 \left[\bar{j} \cdot (\bar{l}_0 \times \bar{n}) \right] dS \qquad (2.6)$$

The determination of the forces and moment thus involves the specification of the body surface geometry, the determination of the normal velocity component ($\bar{U} \cdot \bar{n}$) to the surface area dS and integration over the body surface area which is exposed to the flow.

2.2 Body of Revolution

Consider a body of revolution whose radius, r, is a function of x (Fig. 3). Such a surface is described by

$$g = f(x) - r = 0 \qquad (2.7)$$

and the inward unit normal vector to this surface is

$$\bar{n} = \frac{\bar{\nabla} g}{|\bar{\nabla} g|} \qquad (2.8)$$

Using $r = \sqrt{y^2 + z^2}$ and denoting $df(x)/dx$ by f', the unit normal vector in Cartesian coordinates is

$$\bar{n} = \frac{f f' \bar{i} - y \bar{j} - z \bar{k}}{f \sqrt{1 + (f')^2}} \qquad (2.9)$$

5

In cylindrical coordinates

$$\bar{n} = \frac{f' \bar{\imath} - \bar{u}_\wedge}{\sqrt{1 + (f')^2}} \qquad (2.10)$$

where $\bar{u}_\wedge$ is the unit radial vector (Fig. 3)

The incremental surface area, dS, may be related to its projection, dA, on the cylindrical surface $\wedge\, d\theta\, dx$

$$\left| \bar{u}_\wedge \cdot \bar{n} \right| dS = dA = \wedge\, d\theta\, dx \qquad (2.11)$$

In Eq. 2.11, the absolute magnitude of the dot product was taken because only positive areas are desired. Thus

$$dS = \frac{1}{\left| \bar{u}_\wedge \cdot \bar{n} \right|} \wedge\, d\theta\, dx \qquad (2.12)$$

Substituting Eq. 2.10 into Eq. 2.12, the element of area for a surface of revolution which is described by Eq. 2.7 is

$$dS = f \sqrt{1 + (f')^2} \; d\theta\, dx \qquad (2.13)$$

Restricting motion to the x-z plane, then

$$\bar{\ell}_0 = (x - x_0)\bar{\imath} + y\,\bar{\jmath} + (z - z_0)\bar{k} \qquad (2.14)$$

6

$$\bar{l}_{cg} = (x - x_{cg})\bar{i} + y\bar{j} + (z - z_{cg})\bar{k} \qquad (2.15)$$

$$\bar{\omega} = q\bar{j} \qquad (2.16)$$

$$\overline{V}_{\infty} = V_{\infty}(\cos\alpha \ \bar{i} + \sin\alpha \ \bar{k}) \qquad (2.17)$$

Utilizing Eqs. 2.7, 2.9, 2.14, and

$$z = \Lambda \sin\theta = f\sin\theta \qquad (2.18)$$

the following relations are obtained

$$\bar{i}\cdot\bar{n} = \frac{f'}{\sqrt{1 + (f')^2}}$$

$$\bar{k}\cdot\bar{n} = \frac{-\sin\theta}{\sqrt{1 + (f')^2}} \qquad (2.19)$$

$$\bar{j}\cdot(\bar{l}_0 \times \bar{n}) = \frac{\sin\theta\left[ff' + (x - x_0)\right] - f'z_0}{\sqrt{1 + (f')^2}}$$

7

Substituting $\bar{l}_{ca}$, $\bar{\omega}$, and $\overline{V_{\infty}}$ from Eqs. 2.15, 2.16, and 2.17 into Eq. 2.3, the local flow velocity vector for this planar case is

$$\bar{U} = \left[V_{\infty} \cos\alpha - q(z - z_{ca}) \right] \bar{i} + \left[V_{\infty} \sin\alpha + q(x - x_{cg}) \right] \bar{k} \quad (2.20)$$

and the normal component of this velocity vector to the surface area dS is

$$\bar{U} \cdot \bar{n} = \frac{1}{\sqrt{1 + (f')^2}} \left\{ f' \left[V_{\infty} \cos\alpha - q(f \sin\theta - z_{cg}) \right] \right.$$

$$\left. - \sin\theta \left[V_{\infty} \sin\alpha + q(x - x_{cg}) \right] \right\} \quad (2.21)$$

Also

$$(\bar{U} \cdot \bar{n})^2 = V_{\infty}^2 \left[K_1 - K_2 \sin\theta + K_3 \sin^2\theta \right] \quad (2.22)$$

where

$$K_1 = \frac{(f')^2}{1 + (f')^2} \left[\cos^2\alpha + 2 z_{cg} \left(\frac{q}{V_{\infty}} \right) \cos\alpha \right]$$

$$(2.23)$$

$$K_2 = \frac{f'}{1 + (f')^2} \left[\sin 2\alpha + 2 z_{cg} \left(\frac{q}{V_{\infty}} \right) \sin\alpha - 2 x_{cg} \left(\frac{q}{V_{\infty}} \right) \cos\alpha \right]$$

$$+ \frac{f'(ff' + x)}{1 + (f')^2} \left[2 \left(\frac{q}{V_{\infty}} \right) \cos\alpha \right]$$

8

$$K_3 = \frac{1}{1+(f')^2}\left[\sin^2\alpha - 2\,x_{cG}\left(\frac{q}{V_\infty}\right)\sin\alpha\right]$$

$$+ \frac{ff'+x}{1+(f')^2}\left[2\left(\frac{q}{V_\infty}\right)\sin\alpha\right]$$

In the above, higher order terms involving q^2 were neglected. Substituting Eqs. 2.13, 2.19, and 2.22 into Eq. 2.4 - 2.6, the forces and moment become

$$X = \rho V_\infty^2 \int_{x_1}^{x_2}\int_{\theta_1}^{\theta_2}\left\{f(f')^3\cos^2\alpha - f(f')^2\sin 2\alpha\,\sin\theta\right.$$

$$\left. + ff'\sin^2\alpha\,\sin^2\theta\right\}\frac{dx}{1+(f')^2}\,d\theta \tag{2.24}$$

$$N = \rho V_\infty^2 \int_{x_1}^{x_2}\int_{\theta_1}^{\theta_2}\left\{-f(f')^2\cos^2\alpha\,\sin\theta\right.$$

$$\left. + ff'\sin 2\alpha\,\sin^2\theta - f\sin^2\alpha\,\sin^3\theta\right\}\frac{dx}{1+(f')^2}\,d\theta \tag{2.25}$$

9

$$M = \rho V_\infty^2 \int\limits_{x_1}^{x_2} \int\limits_{\theta_1}^{\theta_2} \left\{ C_1 + C_2 \sin\theta - C_3 \sin\theta + C_4 \sin^3\theta \right\} \frac{dx}{1+(f')^2} \, d\theta \qquad (2.26)$$

where

$$C_1 = -f(f')^3 Z_0 \left[\cos^2\alpha + 2 Z_{CG} \frac{q}{V_\infty} \cos\alpha \right] \qquad (2.27)$$

$$
\begin{aligned}
C_2 = {}& f(f')^2 (ff' + x - x_0) \left[\cos^2\alpha + 2 Z_{CG} \left(\frac{q}{V_\infty}\right) \cos\alpha \right] \\
& + f(f')^2 Z_0 \left[\sin 2\alpha + 2 Z_{CG} \left(\frac{q}{V_\infty}\right) \sin\alpha - 2 X_{CG} \left(\frac{q}{V_\infty}\right) \cos\alpha \right] \\
& + f(f')^2 (ff' + x) Z_0 \left[2 \left(\frac{q}{V_\infty}\right) \cos\alpha \right]
\end{aligned} \qquad (2.28)
$$

$$
\begin{aligned}
C_3 = {}& ff'(ff' + x - x_0) \left[\sin 2\alpha + 2 Z_{CG} \left(\frac{q}{V_\infty}\right) \sin\alpha - 2 X_{CG} \left(\frac{q}{V_\infty}\right) \cos\alpha \right] \\
& + ff'(ff' + x)(ff' + x - x_0) \left[2 \left(\frac{q}{V_\infty}\right) \cos\alpha \right] \\
& + ff' Z_0 \left[\sin^2\alpha - 2 X_{CG} \left(\frac{q}{V_\infty}\right) \sin\alpha \right] \\
& + ff'(ff' + x) Z_0 \left[2 \left(\frac{q}{V_\infty}\right) \sin\alpha \right]
\end{aligned} \qquad (2.29)
$$

$$C_y = f(ff' + x - x_o)\left[\sin^2\alpha - 2 x_{cg}\left(\frac{q}{V_\infty}\right)\sin\alpha\right]$$

$$+ f(ff' + x)(ff' + x - x_o)\left[2\left(\frac{q}{V_\infty}\right)\sin\alpha\right]$$

(2.30)

In obtaining Eq. 2.24 and 2.25, the terms involving the pitching velocity q were neglected because the forces X and N are mainly dependent on the angle of attack α. However, the q terms were retained in the moment expression, Eq. 2.26, since they provide the damping-in-pitch for the vehicle.

The forces and moment can also be expressed in terms of nondimensional coefficients. The defining equations are

$$X = \frac{1}{2}\rho V_\infty^2 S C_x$$

$$N = \frac{1}{2}\rho V_\infty^2 S C_N$$

(2.31)

$$M = \frac{1}{2}\rho V_\infty^2 S d\left[C_M + \frac{d}{2V_\infty}C_{M_q}(q)\right]$$

where C_M is the static moment coefficient, S is an arbitrary reference area, and d is an arbitrary reference diameter.

Assuming the θ limits of integration are independent of x, the x and θ integrations may be performed separately. The consequence resulting from these independent integrations is discussed in Subsection 2.3. Carrying out these operations and comparing terms in Eqs. 2.24 - 2.26 with the corresponding

11

terms in Eqs. 2.31, the following aerodynamic coefficients are obtained:

$$C_X = 2\left(\frac{L^2}{S}\right)\left[A\cos^2\alpha \; \Phi_1 \; - B\sin 2\alpha \; \Phi_2 \; + C\sin^2\alpha \; \Phi_3\right] \qquad (2.32)$$

$$C_N = 2\left(\frac{L^2}{S}\right)\left[-B\cos^2\alpha \; \Phi_2 \; + C\sin 2\alpha \; \Phi_3 \; - D\sin^2\alpha \; \Phi_4\right] \qquad (2.33)$$

$$C_M = 2\left(\frac{L^2}{S}\right)\left(\frac{L}{d}\right)\left[E\cos^2\alpha \; \Phi_2 \; - F\sin 2\alpha \; \Phi_3 \; + G\sin^2\alpha \; \Phi_4\right]$$

$$\qquad (2.34)$$

$$+\left(\frac{L}{d}\right)\left[\left(\frac{x_o}{L}\right)C_N - \left(\frac{z_o}{L}\right)C_X\right]$$

$$C_{M_q} = 8\left(\frac{L^2}{S}\right)\left(\frac{L}{d}\right)^2 \left\{\left[-\left(\frac{z_o}{L}\right)\left(\frac{z_{CG}}{L}\right)A\cos\alpha \; \Phi_1\right]\right.$$

$$+\left\{\left(\frac{z_o}{L} + \frac{z_{CG}}{L}\right)E\cos\alpha + B\left[\left(\frac{z_o}{L}\right)\left(\frac{z_{CG}}{L}\sin\alpha - \frac{x_{CG}}{L}\cos\alpha\right)\right.\right.$$

$$\qquad (2.35)$$

$$\left.\left.-\left(\frac{x_o}{L}\right)\left(\frac{z_{CG}}{L}\right)\cos\alpha\right]\right\}\Phi_2 - \left\{H\cos\alpha + \left[F - \left(\frac{x_o}{L}\right)C\right]\left(\frac{z_{CG}}{L}\sin\alpha - \frac{x_{CG}}{L}\cos\alpha\right)\right.$$

$$\left.-\left(\frac{z_o}{L}\right)\left(\frac{x_{CG}}{L}\right)C\sin\alpha + F\left(\frac{z_o}{L}\sin\alpha - \frac{x_o}{L}\cos\alpha\right)\right\}\Phi_3$$

$$\left.+\left\{-\left(\frac{x_{CG}}{L} + \frac{x_o}{L}\right)G\sin\alpha + \left(\frac{x_o}{L}\right)\left(\frac{x_{CG}}{L}\right)D\sin\alpha + I\sin\alpha\right\}\Phi_4\right\}$$

where L is an arbitrary reference length.

In Eqs. 2.32 - 2.35, the x-integrations, which depend only on the shape of the body surface, are represented by the following:

$$A = \frac{1}{L^2} \int_{x_1}^{x_2} \frac{f(f')^3}{1 + (f')^2} \, dx = \int_{x_1/L}^{x_2/L} \frac{(f/L) \left[\frac{d(f/L)}{d(x/L)} \right]^3}{1 + \left[\frac{d(f/L)}{d(x/L)} \right]^2} \, d\left(\frac{x}{L} \right)$$

Similarly

$$B = \int_{x_1/L}^{x_2/L} \frac{(f/L) \cdot (f')^2}{1 + (f')^2} \, d\left(\frac{x}{L} \right)$$

$$C = \int_{x_1/L}^{x_2/L} \frac{(f/L) \cdot f'}{1 + (f')^2} \, d\left(\frac{x}{L} \right)$$

$$D = \int_{x_1/L}^{x_2/L} \frac{(f/L)}{1 + (f')^2} \, d\left(\frac{x}{L} \right) \qquad\qquad (2.36)$$

$$E = \int_{x_1/L}^{x_2/L} \frac{(f/L)^2 \cdot (f')^3}{1 + (f')^2} \, d\left(\frac{x}{L} \right) + \int_{x_1/L}^{x_2/L} \frac{(f/L) \cdot (f')^2 \cdot (x/L)}{1 + (f')^2} \, d\left(\frac{x}{L} \right)$$

$$F = \int_{x_1/L}^{x_2/L} \frac{(f/L)^2 \cdot (f')^2}{1 + (f')^2} \, d\left(\frac{x}{L} \right) + \int_{x_1/L}^{x_2/L} \frac{(f/L) \cdot f' \cdot (x/L)}{1 + (f')^2} \, d\left(\frac{x}{L} \right)$$

13

$$G = \int_{x_1/L}^{x_2/L} \frac{(f/L)^2 \cdot f'}{1+(f')^2} \, d\left(\frac{x}{L}\right) + \int_{x_1/L}^{x_2/L} \frac{(f/L)\cdot(x/L)}{1+(f')^2} \, d\left(\frac{x}{L}\right)$$

$$H = \int_{x_1/L}^{x_2/L} \frac{(f/L)^3(f')^3}{1+(f')^3} \, d\left(\frac{x}{L}\right) + 2\int_{x_1/L}^{x_2/L} \frac{(f/L)^2(f')^2(\frac{x}{L})}{1+(f')^2} \, d\left(\frac{x}{L}\right) + \int_{x_1/L}^{x_2/L} \frac{(f/L)\cdot f'\cdot(x/L)^2}{1+(f')^2} \, d\left(\frac{x}{L}\right)$$

$$I = \int_{x_1/L}^{x_2/L} \frac{(f/L)^3\cdot(f')^2}{1+(f')^2} \, d\left(\frac{x}{L}\right) + 2\int_{x_1/L}^{x_2/L} \frac{(f/L)^2\cdot f'\cdot(x/L)}{1+(f')^2} \, d\left(\frac{x}{L}\right) + \int_{x_1/L}^{x_2/L} \frac{(f/L)\cdot(x/L)^2}{1+(f')^2} \, d\left(\frac{x}{L}\right)$$

The θ-integrations are given by Φ_1, Φ_2, Φ_3 and Φ_4 below. For a body of revolution, the θ-integration may be carried out over half the body and then doubled

$$\Phi_1 = 2\int_{\theta_1}^{\theta_2} d\theta = 2(\theta_2 - \theta_1)$$

$$\Phi_2 = 2\int_{\theta_1}^{\theta_2} \sin\theta \, d\theta = 2(\cos\theta_1 - \cos\theta_2) \qquad (2.37)$$

$$\Phi_3 = 2\int_{\theta_1}^{\theta_2} \sin^2\theta \, d\theta = \theta_2 - \theta_1 + \frac{\sin 2\theta_1}{2} - \frac{\sin 2\theta_2}{2}$$

14

$$\Phi_4 = 2 \int_{\theta_1}^{\theta_2} \sin^3\theta \, d\theta = 2\left(\cos\theta_1 - \cos\theta_2 + \frac{1}{3}\cos^3\theta_2 - \frac{1}{3}\cos^3\theta_1\right)$$

The θ-integrations are seen to depend on both the body shape (f) and the amount of flow shielding (θ_1, θ_2). This flow shielding is discussed in the following section.

2.3 Flow Shielding

There will be some angles of attack at which portions of the body surface are inclined away from the local velocity direction, (i.e., surfaces which are not exposed to the flow). Newtonian theory assumes that there is no pressure (and hence, no force) on such "shielded" surfaces. Therefore, the limits of integration must be such that shielded areas are excluded, and the integration is carried out only over that portion of the body surface which is exposed to the flow.

The boundary between the shielded and unshielded portions occurs at points where the local velocity $\overline{U}$ is tangent to the body surface. Thus, the surface normal vector, $\overline{n}$, and the local velocity, $\overline{U}$, are perpendicular at the shielding boundary. Hence, the shielding boundary is given by

$$\overline{U} \cdot \overline{n} = 0 \qquad (2.38)$$

where the expression for $\overline{U} \cdot \overline{n}$ is given by Eq. 2.21.

15

The shielding boundary is then determined by setting Eq. 2.21 equal to zero, and obtaining the corresponding value of θ. Denoting this solution as θ_u , then

$$\theta_u = \sin^{-1} \left\{ \frac{f' \left[\cos\alpha + \left(\frac{qL}{V_\infty}\right) \frac{z_{cg}}{L} \right]}{\sin\alpha + \left(\frac{qL}{V_\infty}\right) \frac{(x - x_{cg} + f'f)}{L}} \right\} \qquad (2.39)$$

Thus, the shielding condition is seen to depend on the body shape, the angle of attack, the nondimensional pitch rate term $\left(qL/V_\infty\right)$, and the center-of-gravity location. A great simplification results if the pitching term is neglected. This can be justified in the many cases where $\left(qL/V_\infty\right) \ll 1$. Neglecting the q terms in Eq. 2.39, the shielding boundary reduces to

$$\theta_u = \sin^{-1} \left\{ \frac{f'}{\tan\alpha} \right\} \qquad (2.40)$$

Note that the q terms have also been omitted previously in the force expressions, Eqs. 2.24 and 2.25, but were retained in the moment expression, Eq. 2.26.

It is seen from Eq. 2.40 that the limits on the θ-integration in Eqs. 2.24 - 2.26 are generally a function of x. In obtaining Eqs. 2.32 - 2.35, the limits were taken as invariant with x, making it possible to divide the problem into two independent integrations; an x-integration as in Eqs. 2.36 and a θ-integration as in Eqs. 2.37. Thus when shielding is present, Eqs. 2.32 - 2.35 apply only to a body of revolution where f(x) is a linear function, i.e., a cone, frustum and cylinder, all of which are derivable as special cases of a right circular

16

cone frustum. When no flow shielding exists, Eqs. 2.32 - 2.35 apply to any body of revolution.

For an axially-symmetric body, the shielded portion of the surface is exactly reversed for positive and negative angles of attack (Fig. 4). Using Eq. 2.40 and referring to Fig. 4, the upper and lower limits on θ (θ_1 and θ_2) are summarized below in terms of the argument $f'/\tan\alpha$.

(a) The surface has NO SHIELDING when:

$$\left| \frac{f'}{\tan\alpha} \right| \geq 1 \qquad \text{and} \qquad f' \cos\alpha > 0$$

then $\qquad \theta_1 = -\frac{\pi}{2} \quad , \quad \theta_2 = \frac{\pi}{2}$ $\qquad\qquad$ (2.41a)

(b) The surface is PARTIALLY SHIELDED when:

$$\left| \frac{f'}{\tan\alpha} \right| < 1$$

(1) for positive angles of attack $\left(0° \leq \alpha \leq 180°\right)$; i.e.

$\sin\alpha \geq 0$

then $\quad \theta_1 = -\frac{\pi}{2} \quad , \quad \theta_2 = \sin^{-1}\left(\frac{f'}{\tan\alpha}\right)$ (2.41b)

(2) for negative angles of attack $\left(180° < \alpha < 360°\right)$; i.e.

$\sin\alpha < 0$

then $\quad \theta_1 = \sin^{-1}\left(\frac{f'}{\tan\alpha}\right) \quad , \quad \theta_2 = \frac{\pi}{2}$ $\qquad$ (2.41c)

17

(c)   The surface is COMPLETELY SHIELDED when:

$$\left|\frac{f'}{\tan \alpha}\right| \geq 1 \quad \text{and} \quad f' \cos \alpha \leq 0$$

then

$$\theta_1 = -\frac{\pi}{2} \quad , \quad \theta_2 = -\frac{\pi}{2} \tag{2.41d}$$

Thus, when the body surface is completely shielded from the flow, $\theta_1 = \theta_2$, and

$$\Phi_1 = \Phi_2 = \Phi_3 = \Phi_4 = 0 \tag{2.42}$$

SECTION III

APPLICATION TO SPECIFIC SHAPES

The bodies of revolution which are considered in this report, as a consequence of assuming the θ and x-integrations are independent (i.e., $f(x) =$ const), are a right circular cone frustum, right circular cone, and cylinder.

In applying the results of Section II to a specific body shape, the radius function f of Eq. 2.7 must be specified and the x-integrations A, B, C, ... I, of Eq. 2.36 carried out. Then the shielding condition, Eqs. 2.41, must be determined as a function of α, enabling the θ-integrations, Φ_1, Φ_2, Φ_3, and Φ_4 of Eq. 2.37 to be evaluated. The force and moment coefficients C_X, C_N, C_M, C_{Mq} may then be determined from Eqs. 2.32 - 2.35.

3.1 Frustum of Right Circular Cone

Since the cone and cylinder geometries are derivable from a right circular frustum, the frustum may be selected as the typical nth segment of the composite body.

Consider the frustum of a right circular cone (Fig. 5) where the front and rear bases are not exposed to the flow. For such a body of revolution, the function $f_n(x_n)$, Eq. 2.7, is

$$f_n(x_n) = \Lambda(x_n) = \frac{d_n}{2} + x_n \tan \delta_n$$

$$\frac{f_n}{L} = \frac{1}{2}\left(\frac{d_n}{L}\right) + \left(\frac{x_n}{L}\right)\tan \delta_n \qquad (3.1)$$

19

$$f_n' = \frac{d(f_n/L)}{d(x_n/L)} = \tan \delta_n$$

Substituting into Eqs. 2.36 and integrating over the segment length, L_n,

$$A_n = \int_0^{L_n/L} \frac{\left[\frac{1}{2}(d_n/L) + (x_n/L)\tan\delta_n\right]\tan^2\delta_n \; d(x_n/L)}{\sec^2\delta_n}$$

$$A_n = \frac{1}{2}\sin^2\delta_n \tan\delta_n \left[\left(\frac{d_n}{L}\right)\left(\frac{L_n}{L}\right) + \left(\frac{L_n}{L}\right)^2 \tan\delta_n\right]$$

Similarly, one obtains

$$B_n = \frac{1}{2}\sin^2\delta_n \left[\left(\frac{d_n}{L}\right)\left(\frac{L_n}{L}\right) + \left(\frac{L_n}{L}\right)^2 \tan\delta_n\right]$$

$$C_n = \frac{1}{2}\sin\delta_n \cos\delta_n \left[\left(\frac{d_n}{L}\right)\left(\frac{L_n}{L}\right) + \left(\frac{L_n}{L}\right)^2 \tan\delta_n\right]$$

$$(3.2)$$

$$D_n = \frac{1}{2}\cos^2\delta_n \left[\left(\frac{d_n}{L}\right)\left(\frac{L_n}{L}\right) + \left(\frac{L_n}{L}\right)^2 \tan\delta_n\right]$$

$$E_n = \frac{1}{2}\sin^2\delta_n \left[\frac{1}{2}\left(\frac{d_n}{L}\right)^2\left(\frac{L_n}{L}\right)\tan\delta_n \right.$$

$$\left. + \left(\frac{1}{2} + \tan^2\delta_n\right)\left(\frac{d_n}{L}\right)\left(\frac{L_n}{L}\right)^2 + \frac{2}{3}\frac{\tan\delta_n}{\cos^2\delta_n}\left(\frac{L_n}{L}\right)^3\right]$$

$$F_n = \frac{1}{2} \sin \delta_n \cos \delta_n \left[\frac{1}{2} \left(\frac{d_n}{L}\right)^2 \left(\frac{L_n}{L}\right) \tan \delta_n + \left(\frac{1}{2} + \tan^2 \delta_n\right) \left(\frac{d_n}{L}\right) \left(\frac{L_n}{L}\right)^2 \right.$$
$$\left. + \frac{2}{3} \frac{\tan \delta_n}{\cos^2 \delta_n} \left(\frac{L_n}{L}\right)^3 \right]$$

$$G_n = \frac{1}{2} \cos^2 \delta_n \left[\frac{1}{2} \left(\frac{d_n}{L}\right)^2 \left(\frac{L_n}{L}\right) \tan \delta_n + \left(\frac{1}{2} + \tan^2 \delta_n\right) \left(\frac{d_n}{L}\right) \left(\frac{L_n}{L}\right)^2 \right.$$
$$\left. + \frac{2}{3} \frac{\tan \delta_n}{\cos^2 \delta_n} \left(\frac{L_n}{L}\right)^3 \right]$$

$$H_n = \frac{1}{2} \sin \delta_n \cos \delta_n \left[\frac{1}{4} \left(\frac{d_n}{L}\right)^3 \left(\frac{L_n}{L}\right) \tan \delta_n + \frac{1}{4} \left(\frac{d_n}{L}\right)^2 \left(\frac{L_n}{L}\right)^2 \frac{\tan \delta_n}{\cos^2 \delta_n} \left(2 + \sin^2 \delta_n\right) \right.$$

$$\left. + \frac{1}{3} \left(\frac{d_n}{L}\right) \left(\frac{L_n}{L}\right)^3 \sec^4 \delta_n \left(1 + 2 \sin^2 \delta_n\right) + \frac{1}{2} \left(\frac{L_n}{L}\right)^4 \tan \delta_n \sec^4 \delta_n \right]$$

$$I_n = \frac{1}{2} \cos^2 \delta_n \left[\frac{1}{4} \left(\frac{d_n}{L}\right)^3 \left(\frac{L_n}{L}\right) \tan \delta_n + \frac{1}{4} \left(\frac{d_n}{L}\right)^2 \left(\frac{L_n}{L}\right)^2 \frac{\tan \delta_n}{\cos^2 \delta_n} \left(2 + \sin^2 \delta_n\right) \right.$$

$$\left. + \frac{1}{3} \left(\frac{d_n}{L}\right) \left(\frac{L_n}{L}\right)^3 \sec^4 \delta_n \left(1 + 2 \sin^2 \delta_n\right) + \frac{1}{2} \left(\frac{L_n}{L}\right)^4 \tan \delta_n \sec^4 \delta_n \right]$$

The shielding boundary, Eq. 2.40, is also a function of the body shape. Since $f'_n = \tan \delta_n$, Eqs. 2.41 show that the frustum is completely immersed in the flow (unshielded) when the local angle of attack α_n is less than or equal to the angle δ_n (i.e., when $|\alpha_n| \leq \delta_n$). However, when the angle of attack exceeds the angle δ_n, partial shielding occurs. The amount of this shielding varies with the local angle of attack since

$$\theta_u = \sin^{-1} \left\{ \frac{\tan \delta_n}{\tan \alpha_n} \right\} \tag{3.3}$$

21

The shielding increases with angle of attack until the frustum becomes completely shielded at $\alpha_n \geq \pm (180 - \delta_n)$. Having determined θ_1 and θ_2 from Eqs. 2.41 and Φ_1, Φ_2, Φ_3, Φ_4 from Eqs. 2.37, the force and moment coefficients of the frustum are obtained by substituting Eqs. 3.2 into Eqs. 2.32 - 2.35.

3.2 Right Circular Cone

The cone case is obtained directly from the frustum by setting the front base diameter d_n equal to zero in Eqs. 3.2. The procedure involved in obtaining C_X, C_N, C_M, C_{Mq} for the cone is then exactly as outlined in Subsection 3.1.

For the purpose of illustrating the procedure, closed-form expressions are derived for the simple case of small angles of attack. For a cone, Eq. 3.1 gives

$$\frac{d_c}{2} = L_n \tan \delta \qquad (3.4)$$

where d_c is the cone base diameter, L_n is the cone length, and δ is the cone half angle. Since L, S, and d appearing in Eqs. 2.32 - 2.35 are arbitrary reference quantities, they may be selected as

$$L = L_n$$

$$S = \frac{\pi d_c^2}{4} \qquad (3.5)$$

$$d = d_c$$

Thus

$$\frac{L^2}{S} = \frac{1}{\pi \tan^2 \delta}$$

$$\frac{L}{d} = \frac{1}{2 \tan \delta}$$

(3.6)

For simplicity, the cone will be assumed completely immersed in the flow. Thus, for small angles of attack ($|\alpha| \leq \delta$), when no shielding takes place, Eqs. 2.41 give

$$\theta_1 = -\frac{\pi}{2}$$

$$\theta_2 = \frac{\pi}{2}$$

(3.7)

and Eqs. 2.37 give

$$\Phi_1 = 2\pi$$

$$\Phi_2 = \Phi_4 = 0$$

(3.8)

$$\Phi_3 = \pi$$

for both $+\alpha$ and $-\alpha$. Substituting Eqs. 3.2, with $d_n = 0$ and $L_n/L = 1$, into Eqs. 2.32 - 2.35 and using Eqs. 3.6 and 3.8, the force and moment coefficients of the cone for small α (unshielded) are

23

$$C_X = 2 \sin^2 \delta + \sin^2 \alpha \, (1 - 3 \sin^2 \delta)$$

$$C_N = \cos^2 \delta \, \sin 2\alpha$$

(3.9)

$$C_M = \cot \delta \, \sin 2\alpha \left[-\frac{1}{3} + \frac{1}{2} \left(\frac{x_o}{L} \right) \cos^2 \delta \right]$$

$$C_{Mq} = -\cot^2 \delta \, \cos \alpha \left[\frac{1}{2} \sec^2 \delta - \frac{2}{3} \left(\frac{x_o}{L} + \frac{x_{cg}}{L} \right) - \left(\frac{x_o}{L} \right) \left(\frac{x_{cg}}{L} \right) \cos^2 \delta \right]$$

It should be noted that in Eq. 3.9 the cone is pitching about the center of gravity $(x_{cg}, 0, 0)$ with an angular velocity q, and that C_M and C_{Mq} are both given with respect to the point $(x_o, 0, 0)$.

3.3 Cylinder

A cylinder is easily derived from the frustum case by setting the angle $\delta_n = 0$. Most of the x-integrations in Eqs. 2.36 are zero. Those remaining are

$$D_n = \frac{1}{2} \left(\frac{d_n}{L} \right) \left(\frac{L_n}{L} \right)$$

$$G_n = \frac{1}{4} \left(\frac{d_n}{L} \right) \left(\frac{L_n}{L} \right)^2$$

(3.10)

$$I_n = \frac{1}{6} \left(\frac{d_n}{L} \right) \left(\frac{L_n}{L} \right)^3$$

24

The shielding boundary for the cylinder becomes $\dot{\theta}_u = 0$ since $f_n' / \tan \alpha_n = 0$. This means that either the lower half or the upper half of the cylinder is exposed to the flow, depending on whether the angle of attack α_n is positive or negative.

3.4 Flat Circular Base

Section II dealt with a body of revolution whose radius is a function of the axial distance x. In this section, the equations are derived for a surface which is not a function of x. The surface considered here is a flat circular base that is perpendicular to the x-direction (Fig. 6).

Assuming the flow strikes the rear surface of the base, the inward unit normal vector is

$$\bar{n} = -\bar{i} \tag{3.11}$$

The forces and moments on the surface are again given by Eqs. 2.4 - 2.6, where now

$$\bar{i} \cdot \bar{n} = -1$$

$$\bar{k} \cdot \bar{n} = \bar{k} \cdot (-\bar{i}) = 0 \tag{3.12}$$

$$\bar{j} \cdot \bar{\ell}_0 \times \bar{n} = -\lambda \sin \theta + z_0$$

and

$$\bar{U} \cdot \bar{n} = -V_\infty \left[\cos \alpha - \frac{\dot{q}}{V_\infty} \left(\lambda \sin \theta - z_{cg} \right) \right] \tag{3.13}$$

25

After dropping the higher order q^2 term, as in Eq. 2.22,

$$(\bar{U} \cdot \bar{n})^2 = V_\infty^2 \left[\cos^2\alpha - 2\frac{q}{V_\alpha} \cos\alpha \left(\lambda \sin\theta - z_{ca}\right) \right] \qquad (3.14)$$

The flat base is taken to be circular since only bodies of revolution are considered. Using polar coordinates, the area dS is

$$dS = \lambda \, d\lambda \, d\theta \qquad (3.15)$$

The shielding boundary is given by $(\bar{U} \cdot \bar{n}) = 0$ as in Eq. 2.38. Setting Eq. 3.13 equal to zero and neglecting the q term as in Eq. 2.40, the shielding boundary for the base is

$$\cos\alpha = 0 \qquad (3.16)$$

for nonzero V_∞. A flat base which has only the rear surface exposed to the flow is thus completely shielded when

$$-\frac{\pi}{2} \leq \alpha \leq \frac{\pi}{2} \qquad (3.17)$$

and is completely exposed for all other α.

When the base is exposed $\left(90° < \alpha < 270°\right)$, the forces on the base are obtained by putting Eqs. 3.12, 3.14, and 3.15 into Eqs. 2.4 - 2.6, obtaining

$$X = \rho V_\infty^2 \int_0^{\frac{d_\beta}{2}} \int_0^{2\pi} -\cos^2\alpha \, r \, dr \, d\theta$$

$$N = 0 \tag{3.18}$$

$$M = \rho V_\infty^2 \int_0^{\frac{d_\beta}{2}} \int_0^{2\pi} (C_5 + C_6 \sin\theta + C_7 \sin^2\theta) \, r \, dr \, d\theta$$

where, as in Eqs. 2.24 - 2.26, the q terms have been dropped from the X-force equation for the base, but have been retained in the moment equation. In the M-equation above,

$$C_5 = z_0 \cos^2\alpha + 2 z_0 z_{CG} \left(\frac{q}{V_\infty}\right) \cos\alpha$$

$$C_6 = -r \left[\cos^2\alpha + 2 z_{CG} \left(\frac{q}{V_\infty}\right) \cos\alpha + 2 z_0 \left(\frac{q}{V_\infty}\right) \cos\alpha \right] \tag{3.19}$$

$$C_7 = 2 r^2 \left(\frac{q}{V_\infty}\right) \cos\alpha$$

Integrating Eqs. 3.18 and nondimensionalizing as in Eqs. 2.31, the aerodynamic coefficients for the circular base are

$$C_N = 0$$

$$C_X = -\frac{\pi}{2} \left(\frac{L^2}{S}\right) \left(\frac{d_\beta}{L}\right)^2 \cos^2\alpha \tag{3.20}$$

$$C_M = \frac{\pi}{2} \left(\frac{L^2}{S}\right) \left(\frac{L}{d}\right) \left(\frac{d_\beta}{L}\right)^2 \left(\frac{z_0}{L}\right) \cos^2\alpha$$

27

$$C_{M_{\theta}} = 2\pi \left(\frac{L^2}{S}\right)\left(\frac{L}{d}\right)^2\left(\frac{d_\theta}{L}\right)^2 \cos\alpha \left[\left(\frac{z_\circ}{L}\right)\left(\frac{z_{cG}}{L}\right) + \frac{1}{16}\left(\frac{d_\theta}{L}\right)^2\right]$$

A circular base which has its front surface exposed to the flow is unshielded for $(90° > \alpha > 270°)$. For this case $\bar{n} = +\bar{\iota}$ and the forces and moment expressions in Eqs. 3.20 still apply with a change in sign.

SECTION IV

COMPOSITE BODIES

The body shapes which were discussed in Section III (all derivable as special cases of a right circular cone frustum) may be combined appropriately to form a composite body. For example, the axisymmetric composite body of Fig. 8 (solid lines) consists of a cone, frustum, cylinder, another frustum and finally a circular base. These same five segments can also be used to form an asymmetric body (dashed lines) by rotating each segment through an angle β_n with respect to the principal body axis, x. For convenience, the principal body axis, x, has been selected to coincide with the x_n axis of the rear frustum (segment n = 4), but this is not a necessity.

The total forces and moment on a composite body may be found by summing the contributions due to a number of independent segments. However, within the present scheme for calculating the aerodynamic coefficients for a composite body, there are two problems: (1) when an asymmetric body is formed as shown in Fig. 8, an unrealistic gap-overlap region occurs at the junction of segments rotated relative to each other and (2) for both axisymmetric and asymmetric composite bodies, the presence of mutual shielding, in which one segment shields another from the flow, has been neglected. These two effects have been investigated to some extent in Ref. 6 and are discussed in the following paragraphs.

Only the general shape of an asymmetric body is achieved by rotating and translating segments as indicated. Since the segments considered are right circular cone frusta, they will not join smoothly if one segment is rotated relative to another.

29

It would be possible to connect the rotated frusta by an additional segment at their junction, but such a segment would require a more complex mathematical shape than has been considered. Instead, this report uses a less complicated approach in which the segments are rotated as shown in Fig. 8, resulting in an overlap of areas on one side and a gap on the other side of the junction.

Reference 6 shows that, for small break angles ($|\beta| < 5^{\circ}$) for a bent cone, the coefficients obtained by rotating the segments in this manner differ only slightly from values obtained using a better approximation to the break region. For small break angles, it was found that the several means for accounting more realistically for the "former" gap-overlap region resulted in aerodynamic coefficients which differed very little from each other. As the break angle increases, the bend region should be treated more realistically than indicated in Fig. 8 if theoretically-accurate aerodynamic coefficients are to be predicted.

Some caution must also be used with regard to "mutual shielding" when composite bodies are formed. In Section III, the forces and moment on independent body-of-revolution segments were found by using the shielding criterion,

$$\left(\bar{U} \cdot \bar{n}\right) = 0 \qquad (4.1)$$

However, when dealing with composite bodies, an additional type of shielding may occur when one segment shields another segment from the flow. An example of this "mutual" shielding is shown in Fig. 7. When $\alpha < \delta_1 < \delta_2$, both the cone and the frustum segments are completely exposed to the flow and no mutual shielding occurs. As the angle of attack increases ($\delta_1 < \alpha < \delta_2$), the cone

30

segment becomes independently shielded along the boundary AB, according to Eq. 4.1. Although Eq. 4.1 states that the frustum is completely unshielded until $\alpha > \delta_2$, in reality, the cone will block part of the flow and result in a mutually shielded region, BC, on the frustum. When $\alpha > \delta_2$, independent shielding of the frustum will begin and will partially account for the mutual shielding. Thus, there will be a range of angles of attack for which the direct addition of independent segments to form a composite body will be in error since the shielding of some segments is partially determined by the position of preceding segments instead of by the local normal vector. The extent of this mutual shielding error will depend upon the number and type of the segments and their rotation angles, β_n.

Another body possessing mutual shielding is the bent cone of Fig. 9. Mutual shielding first occurs when the rotated cone segment casts a shadow onto the rear frustum segment $(\alpha = \delta + \beta)$ although the frustum is not independently shielded until $\alpha = \pm \delta$. When the angle of attack reaches 90°, mutual shielding ceases.

The assumption of independent segments causes another error when the flow strikes the bent cone from the rear such that the tip of the cone segment begins to appear over the edge of the flat base. As an independent segment, the rotated cone segment becomes unshielded at $\alpha = \pi + (\delta + \beta)$; however, the tip does not actually become visible to the flow until $\alpha = \pi + \epsilon$, where $\tan \epsilon = (\tan \delta + \frac{L_1}{L} \sin \beta)/(\frac{L_1}{L} \cos \beta + \frac{L_2}{L})$. Most of this premature unshielding has disappeared when $\alpha = \pi + \delta$ but the segments are not strictly independent until $\alpha = 270^{\circ}$. Reference 6 presents a limited numerical assessment of the mutual shielding effect on a bent cone which shows that for $|\beta| < 5^{\circ}$ the effect is very small and limited to a small range of angle of attack. Of course, as β increases, mutual shielding can be expected to become more important.

31

Consider a body composed of N segments ($n = 1, 2, \ldots, N$). Each segment will be considered to be a special case of the typical right-circular-cone frustum which is shown rotated and translated with respect to the principal x-z axis system in Fig. 5. For each segment, d_n/L, L_n/L, δ_n, and β_n must be specified in order to evaluate the coefficients A_n, B_n, $\ldots$, I_n ($n = 1, \ldots, N$) in Eq. 3.2. Following the procedure outlined in Section III, the forces and moment for the nth segment are obtained from Eqs. 2.32-2.35. For example, C_M for segment n is

$$C_M^{(n)} = 2\left(\frac{L^2}{S}\right)\left(\frac{L}{d}\right)\left[E_n \cos^2\alpha_n \, \Phi_2^{(n)} - F_n \sin 2\alpha_n \, \Phi_3^{(n)} \right.$$
$$\left. + G_n \sin^2\alpha_n \, \Phi_4^{(n)}\right] + \left(\frac{L}{d}\right)\left[\frac{(x_o)_n}{L} C_N^{(n)} - \frac{(z_o)_n}{L} C_X^{(n)}\right] \qquad (4.2)$$

where L, S, and d are arbitrary reference quantities, $(x_o)_n$, $(z_o)_n$ are the coordinates of (x_o, z_o) in the $x_n - z_n$ plane and α_n is the local angle of attack for the nth segment, that is

$$\alpha_n = \alpha - \beta_n \qquad (4.3)$$

where α is the angle of attack of the composite body with respect to the principal x-axis.

Through a translation and rotation of axes, any point (x,z) given in the principal body axis system has coordinates (x_n, z_n) in the axis system attached to each segment:

32

$$\frac{X_n}{L} = \left[\frac{x}{L} - \frac{(x_T)_n}{L}\right]\cos\beta_n + \left[\frac{z}{L} - \frac{(z_T)_n}{L}\right]\sin\beta_n$$

$$\tag{4.4}$$

$$\frac{z_n}{L} = \left[\frac{z}{L} - \frac{(z_T)_n}{L}\right]\cos\beta_n - \left[\frac{x}{L} - \frac{(x_T)_n}{L}\right]\sin\beta_n$$

where $(x_T)_n$, $(z_T)_n$ are specified coordinates locating the origin of the $X_n - Z_n$ system. Equations 4.4 are used to transform the points x_o, z_o and x_{cg}, z_{cg} into the segment coordinate axis system. In this way, the moment due to each segment is always taken about the same point (x_o, z_o).

The forces $C_X^{(n)}$ and $C_N^{(n)}$ as calculated by Eqs. 2.32 and 2.33 are directed along the X_n and Z_n axes. These components may be resolved into components along the principal body axes, x, z. Denoting by $C_{X_R}^{(n)}$ and $C_{N_R}^{(n)}$ the components directed along the principal axes (Fig. 5),

$$C_{X_R}^{(n)} = C_X^{(n)} \cos\beta_n - C_N^{(n)} \sin\beta_n$$

$$\tag{4.5}$$

$$C_{N_R}^{(n)} = C_X^{(n)} \sin\beta_n + C_N^{(n)} \cos\beta_n$$

Finally, the total forces and moment acting on the composite body are obtained by summing the contributions due to each segment :

$$\left(C_{X_R}\right)_{TOT} = \sum_{n=1}^{N} C_{X_R}^{(n)}$$

33

$$\left(C_{N_R}\right)_{TOT} = \sum_{n=1}^{N} C_{N_R}^{(n)}$$

$$\left(C_M\right)_{TOT} = \sum_{n=1}^{N} C_M^{(n)}$$

$$\left(C_{M_q}\right)_{TOT} = \sum_{n=1}^{N} C_{M_q}^{(n)}$$

It may be convenient to resolve these forces from body axes to wind axes. If this is desired, the total drag and lift on the body are

$$\left(C_D\right)_{TOT} = \left(C_{N_R}\right)_{TOT} \sin\alpha + \left(C_{X_R}\right)_{TOT} \cos\alpha$$

(4.7)

$$\left(C_L\right)_{TOT} = \left(C_{N_R}\right)_{TOT} \cos\alpha - \left(C_{X_R}\right)_{TOT} \sin\alpha$$

SECTION V

NUMERICAL APPLICATION

The computer program embodying the foregoing analysis is presented in Appendix A and has been used to calculate the aerodynamic coefficients for the example composite bodies presented in Fig. 9. The first body consists of three segments, a cone, cone frustum and circular base; the cone segment is rotated about the 80 and 20 percent body stations. When $\beta = 0$, the resulting body is a 10° cone. The second body consists of four segments, a cone, cylinder, frustum and a circular base where the cone-cylinder combination is rotated arbitrarily about the 79 percent body stations. Figures 10 - 18 present the numerical results as a function of the angle β for the vehicles pitching about the point $X_o = X_{cg}$, $z_o = z_{cg}$.

The results for the cone "broken" at the 80 percent body station show that C_X, C_N, C_M, and C_{Mq} are significantly affected by β. At angles of attack less than approximately 40° (Fig. 11), C_N increases significantly as the cone segment is rotated upward (β is defined positive counter-clockwise); $(C_N)_{MAX}$, however, is seen to decrease. The axial force coefficient, Fig. 10, also increases significantly for $\alpha \leq 100^o$. The increases in the coefficients are attributed to the increased local angle of attack ($\alpha - \beta$) of the cone segment in these angle-of-attack ranges. The effect on C_M, Fig. 12, is to increase the $\alpha = 0$ value and to increase the trim angle of attack, α_T . Thus, a cone "broken" (nose up) at the 80 percent station will experience both a greater normal force and increased drag, and will be flying at a higher trim angle of attack than an "unbroken" cone ($\beta = 0$). The effect on the resulting flight trajectory could be significant. The effect on the pitch-damping behavior is in the direction of increased dynamic stability since C_{Mq}

35

increases negatively for $\alpha \lesssim 80^{\circ}$, (Fig. 13).

For the cone "broken" at the 20 percent station, however, calculations show that the changes in the forces on the rotated tip are too small to influence C_X, C_N, and C_{Mq} significantly. However, since these changes in force are located away from the C.G., C_M shows a distinct dependence on β (Fig. 14).

The results for the cone-cylinder-flare body are the same, qualitatively, as for the 80 percent cone case and are given in Figs. 15 - 18.

Figures 19 and 20 summarize the effect of β on the trim angle of attack and the trim lift-drag ratio. The trim angle of attack is increased appreciably as $-\beta$ increases, for each configuration. The $(L/D)_T$ increases, reaches a maximum, and then decreases. Thus, these configurations may have significant L/D at the trim condition for relatively small values of β.

SECTION VI

CONCLUSIONS

Newtonian impact theory was used to obtain expressions for the static and dynamic aerodynamic coefficients of bodies composed of bodies of revolution. The resulting combined body possesses one plane of symmetry and motion was restricted to that plane.

When the angle of attack is sufficiently small such that no flow shielding is present, the developed expressions (Eqs. 2.32 - 2.35) apply to any segment body of revolution. However, at sufficiently large angles of attack when shielding is present, the limits of integration are not independent, and the developed expressions are restricted to right-circular-cone frusta.

In combining the segment frusta to obtain a composite body, the effects of mutual shielding and any gap-overlap regions have been neglected. Reference 6 shows that, for a bent cone, these two effects appear to be negligible for small asymmetries.

A computer program was developed to calculate the coefficients C_X, C_N, C_M, C_{Mq} for motion in the plane of symmetry for the case where the composite body segments are right circular cone frusta. The complete angle of attack range was considered, and the center of gravity and the moment reference points can both be arbitrary in the plane of symmetry.

Example calculations are given for a body consisting of a cone, cone frustum and circular base, and for a body consisting of a cone, cylinder, cone frustum and a circular base. It was shown that significant changes in the trim angle of attack and lift to drag ratio may result because of the asymmetry of the body.

REFERENCES

1. Reid, Robert C., Jr., and Mayo, Edward W., _Equations for the Newtonian Static and Dynamic Aerodynamic Coefficients for a Body of Revolution with an Offset Center-of-Gravity Location_, NASA TN D-1085, June 1963.

2. Wells, William R., and Armstrong, William O., _Tables of Aerodynamic Coefficients Obtained From Developed Newtonian Expressions for Complete and Partial Conic and Spheric Bodies at Combined Angles of Attack and Sideslip with Some Comparisons with Hypersonic Experimental Data_, NASA TR R-127, 1962.

3. Fisher, Lewis R., _Equations and Charts for Determining the Hypersonic Stability Derivatives of Combinations of Cone Frustums Computed by Newtonian Impact Theory_, NASA TN D-149, 1 November 1959.

4. Visich, Marian, Jr., and Schneider, Jesse, _Aerodynamic Characteristics of a Canted-Cone Re-Entry Body at Hypersonic Velocities (U)_, GASL TR 415, 2 March 1964, SECRET.

5. Schneider, J., Visich, M., Jr., and Schuster, L., _Additional Aerodynamic Characteristics of a Canted-Cone Re-Entry Body at Hypersonic Velocities (U)_, GASL TR 456, 20 July 1964, SECRET.

6. Coulter, D.A., _Newtonian Static and Dynamic Aerodynamic Coefficients for Asymmetric Bodies under Combined Angles of Attack and Sideslip,_ MIT ASRL TR 121-10, to be published. Also, MIT S.M. Thesis, Department of Aeronautics and Astronautics, January 1965.
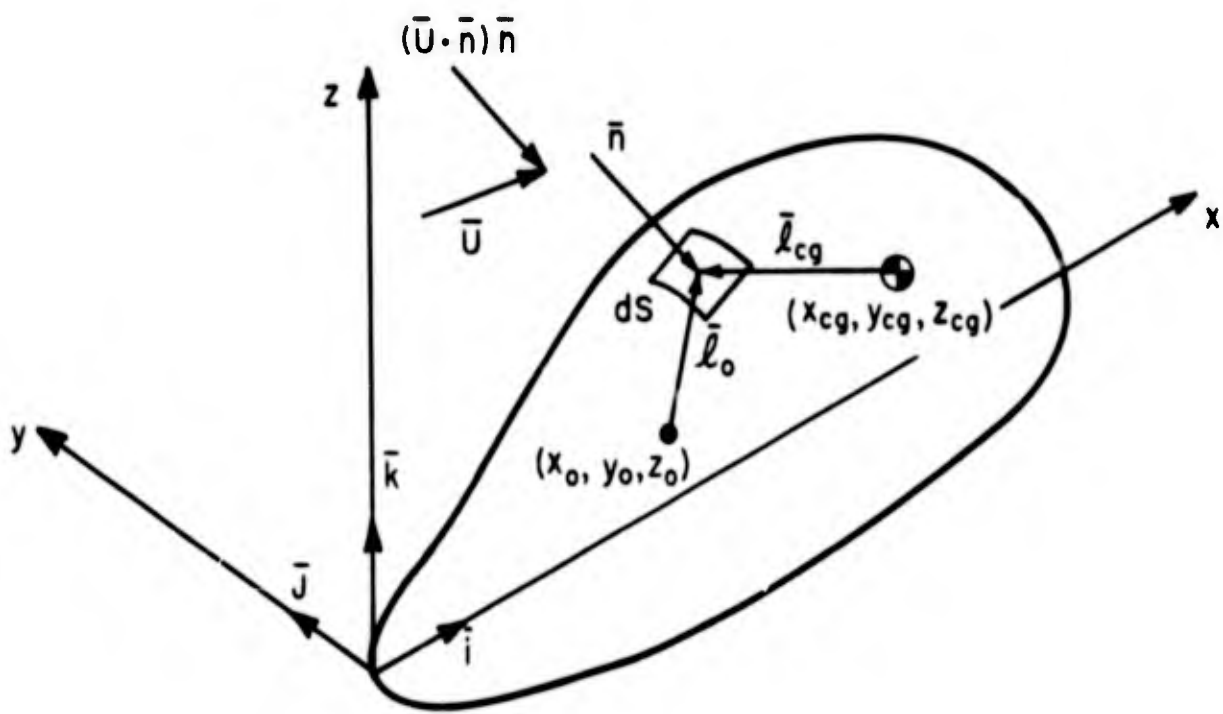
FIG. 1 GENERAL BODY COORDINATE SYSTEM
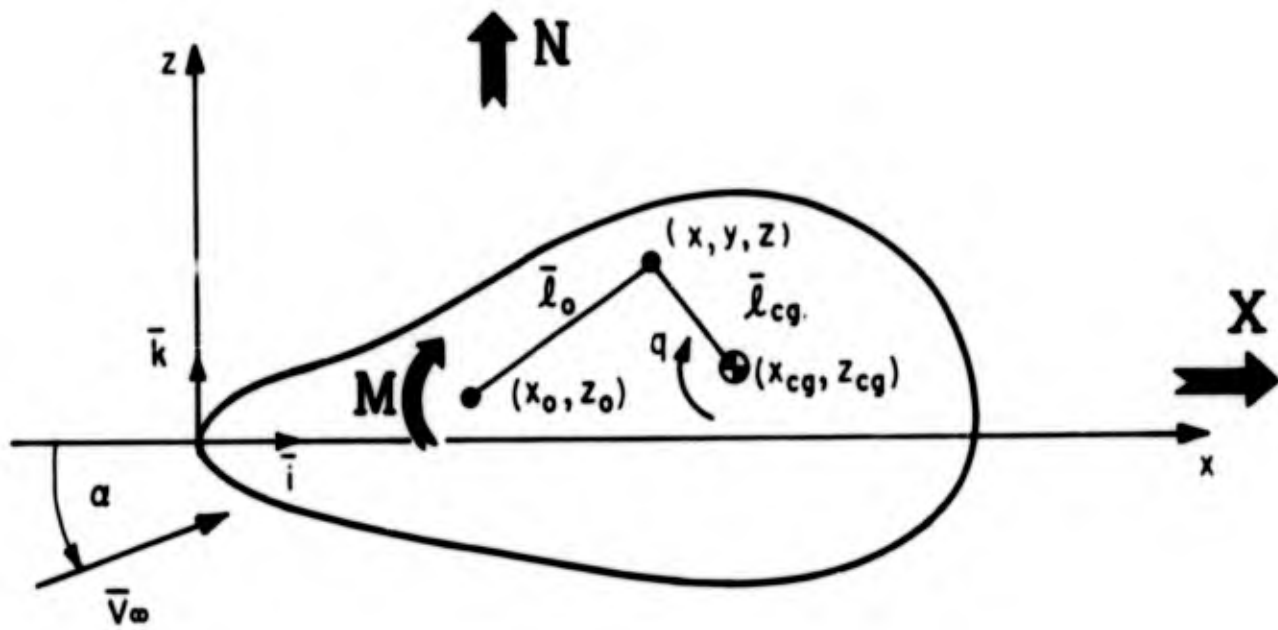
FIG. 2 COORDINATE SYSTEM AND FORCE
NOTATION IN x-z PLANE
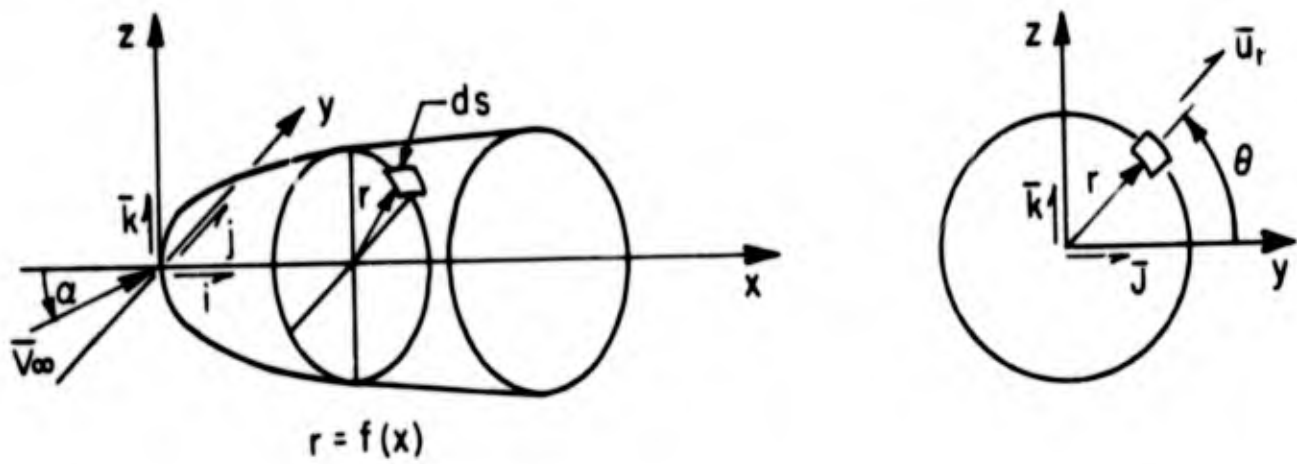
FIG. 3   BODY OF REVOLUTION GEOMETRY
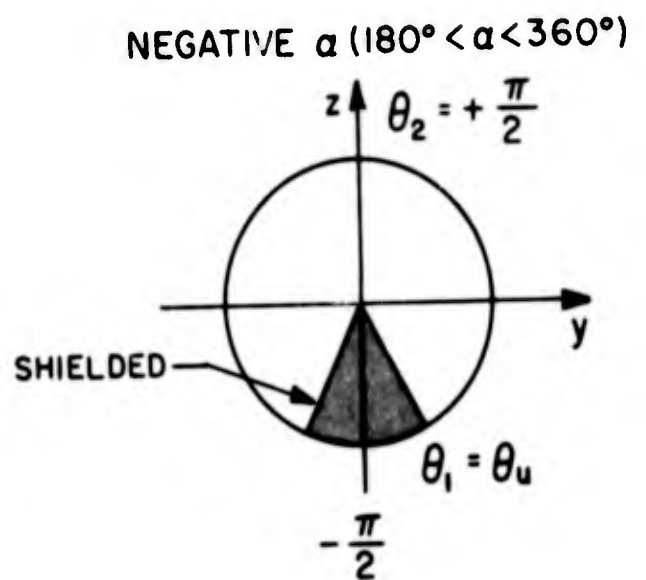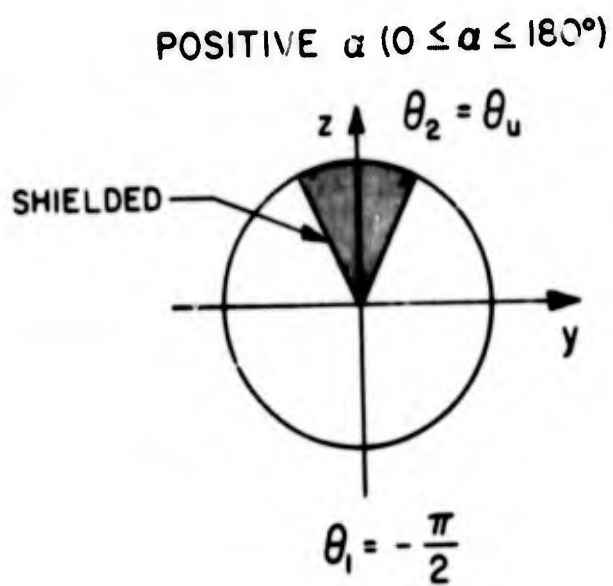
FIG. 4   SHIELDING BOUNDARY FOR BODY OF REVOLUTION
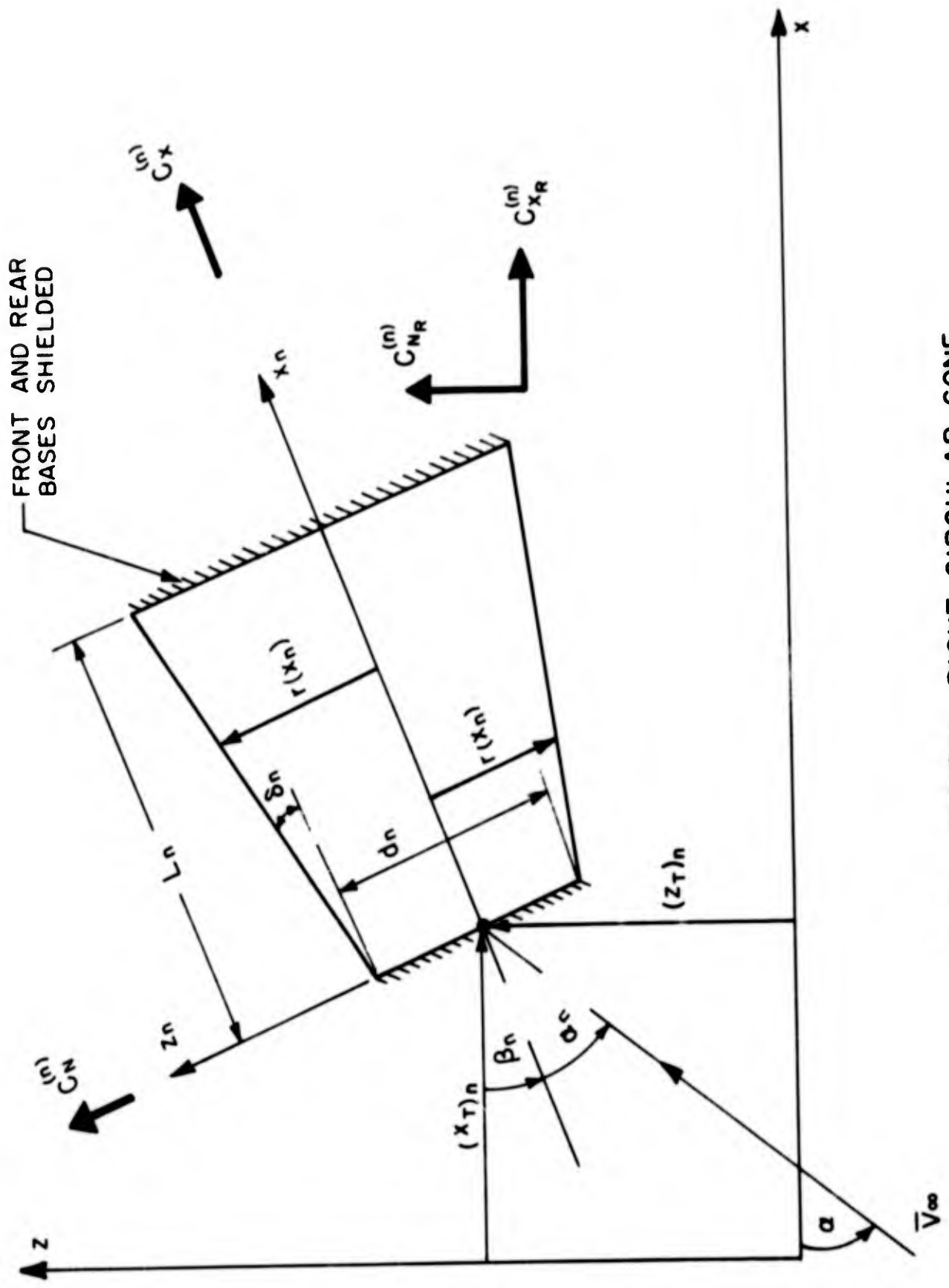
FIG. 5 TYPICAL RIGHT CIRCULAR CONE FRUSTUM SEGMENT NOTATION

41
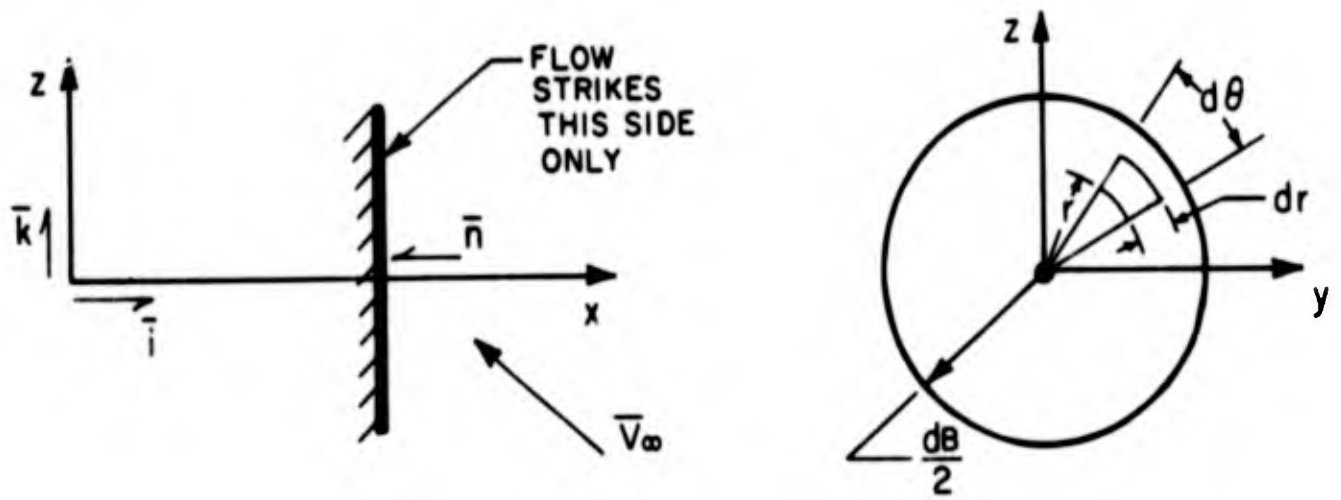
FIG. 6 CIRCULAR BASE GEOMETRY
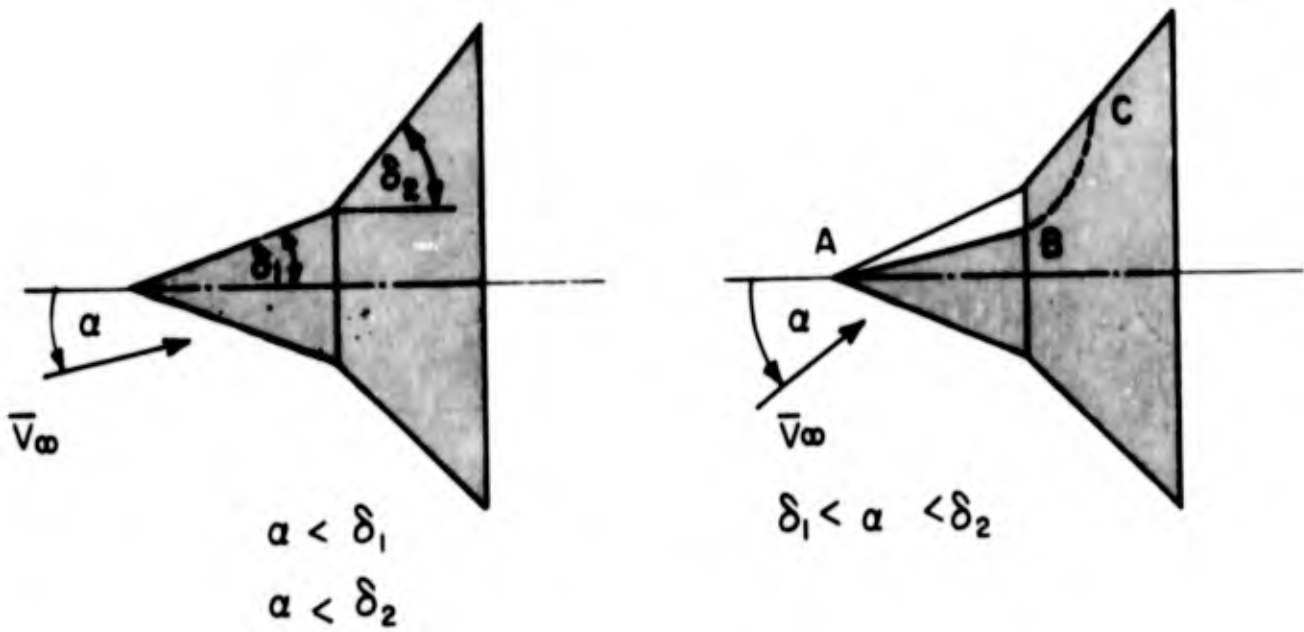
FIG. 7 MUTUAL SHIELDING EFFECT

42
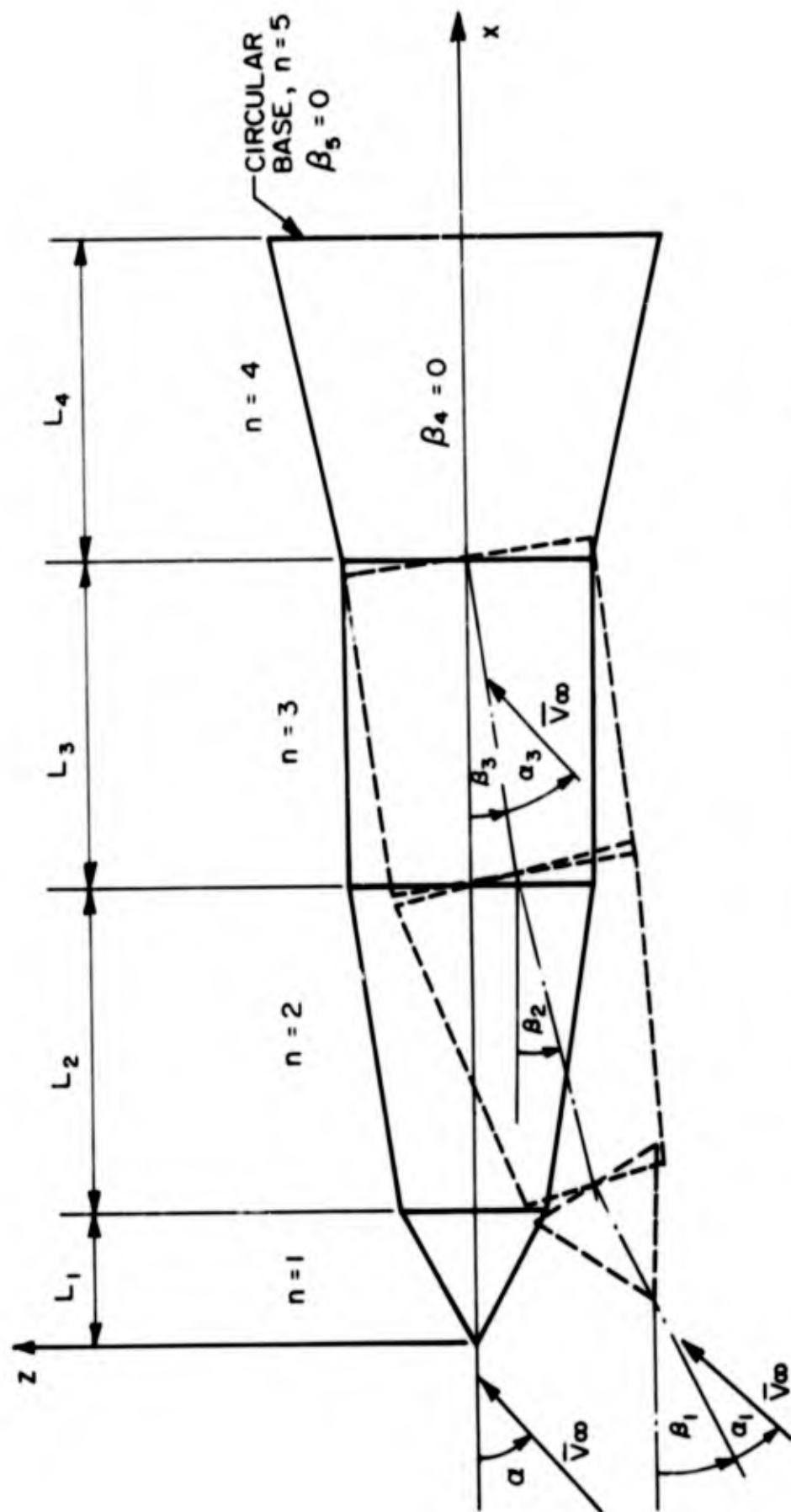
FIG. 8 COMPOSITE BODY OF 5 SEGMENTS
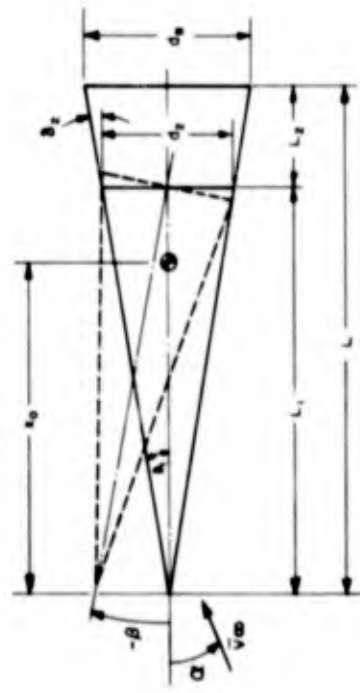
43

FIG. 9 EXAMPLE VEHICLES

FIG. IO AXIAL FORCE COEFFICIENT C_x ~ "BROKEN" CONE, $L_1/L = .8$

45
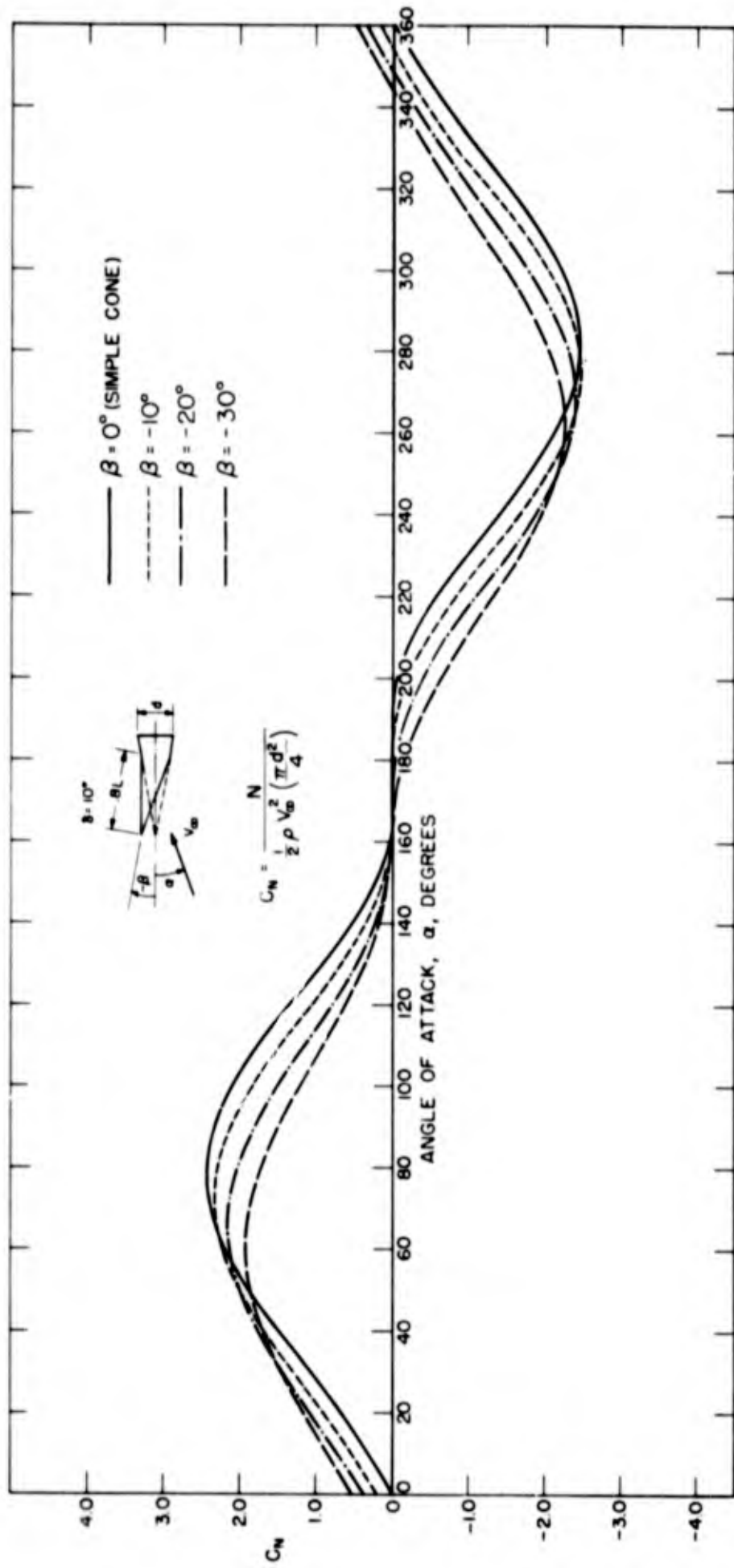
FIG. II   NORMAL FORCE COEFFICIENT $C_N \sim$ "BROKEN" CONE, $\frac{L_1}{L} = .8$
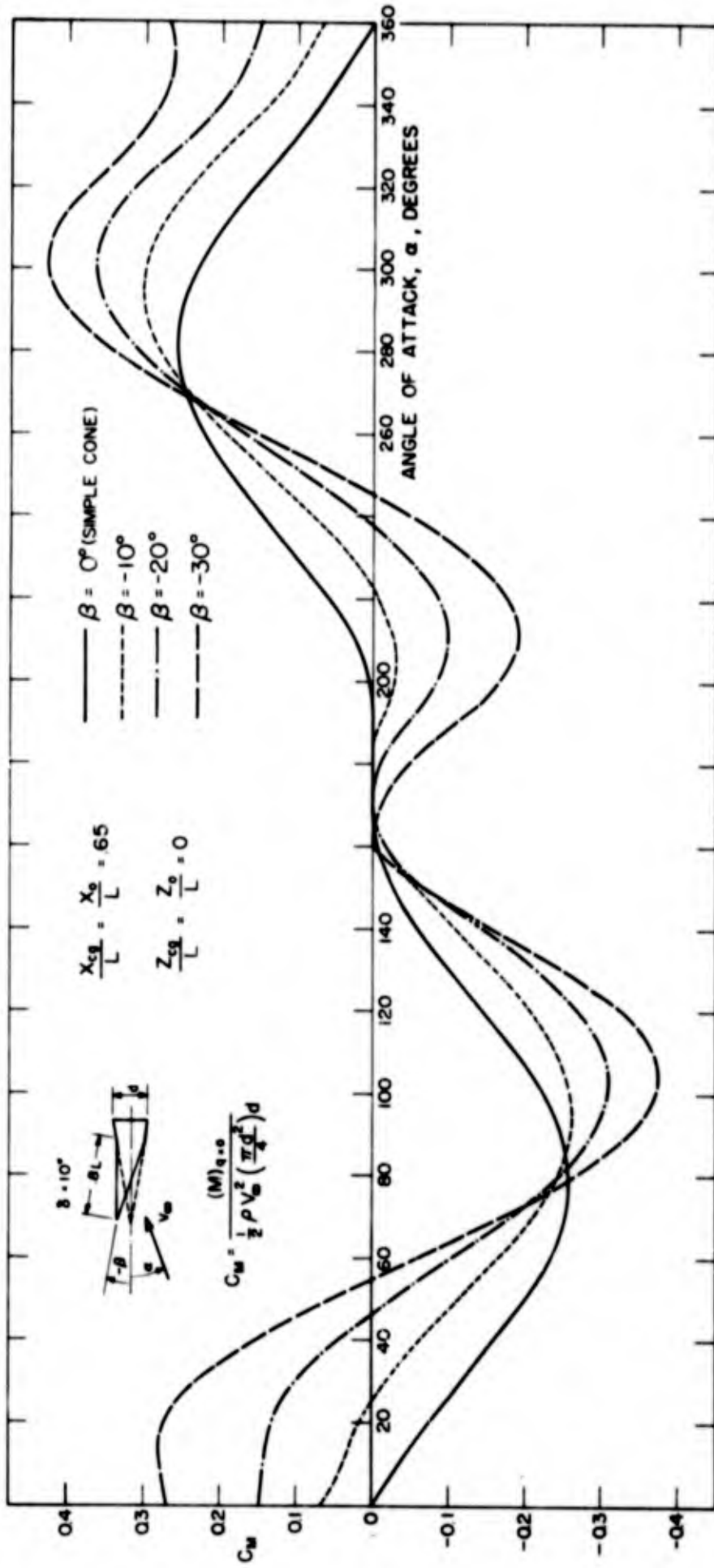
FIG. 12 STATIC PITCHING MOMENT COEFFICIENT $C_M \sim$ "BROKEN" CONE, $L_1/L = .8$
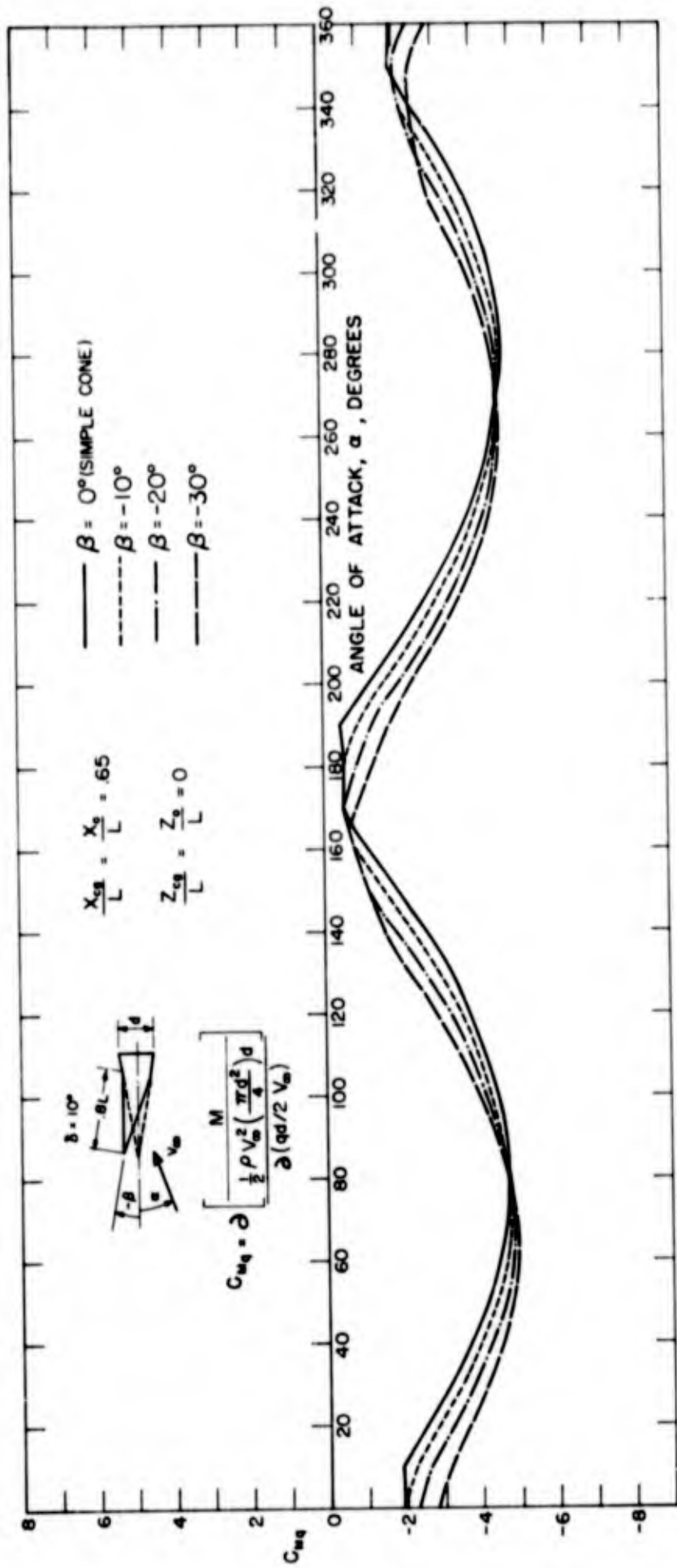
FIG. 13 PITCH DAMPING COEFFICIENT C_{m_q} ~ "BROKEN" CONE, $L_1/L = .8$
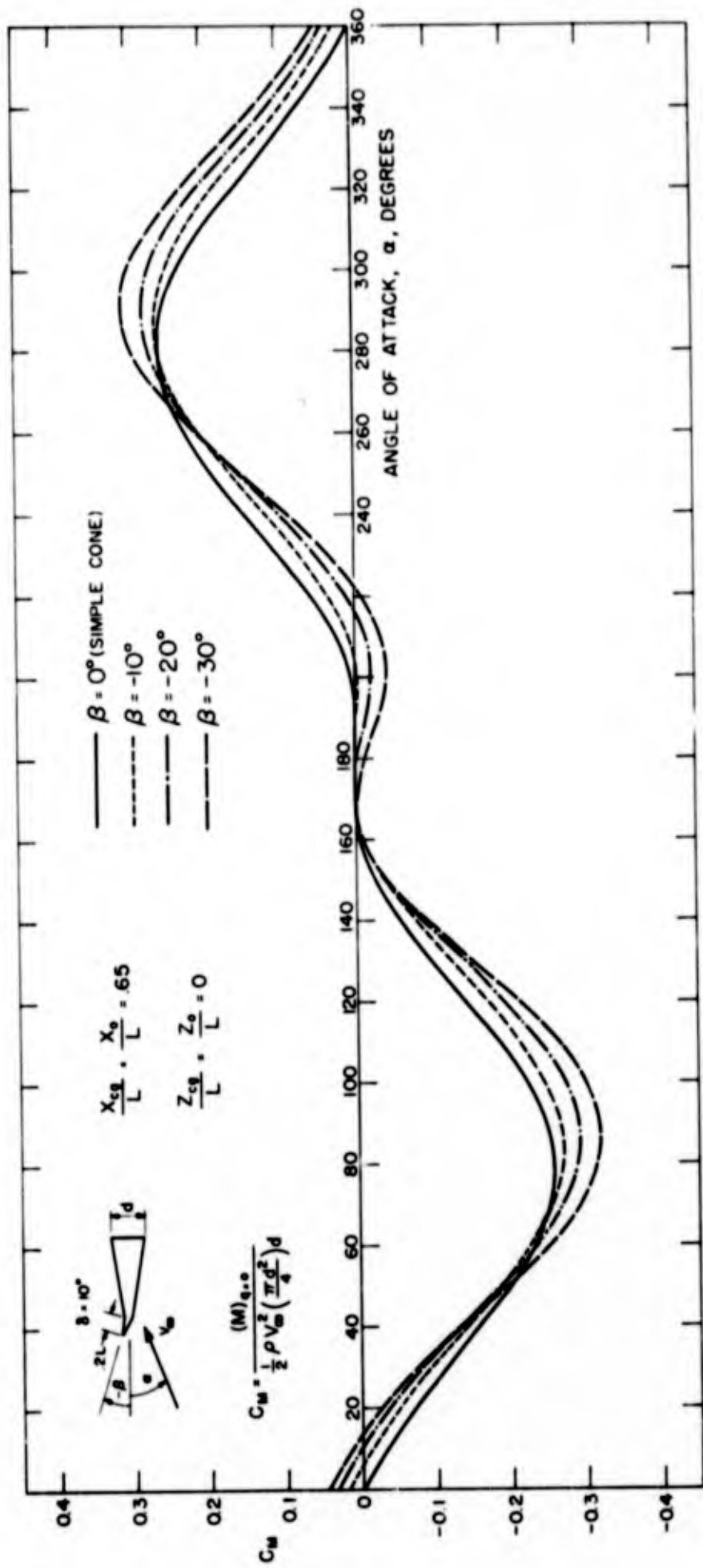
FIG. 14 STATIC PITCHING MOMENT COEFFICIENT C_M ~ "BROKEN" CONE, $L_1/L = .2$

49
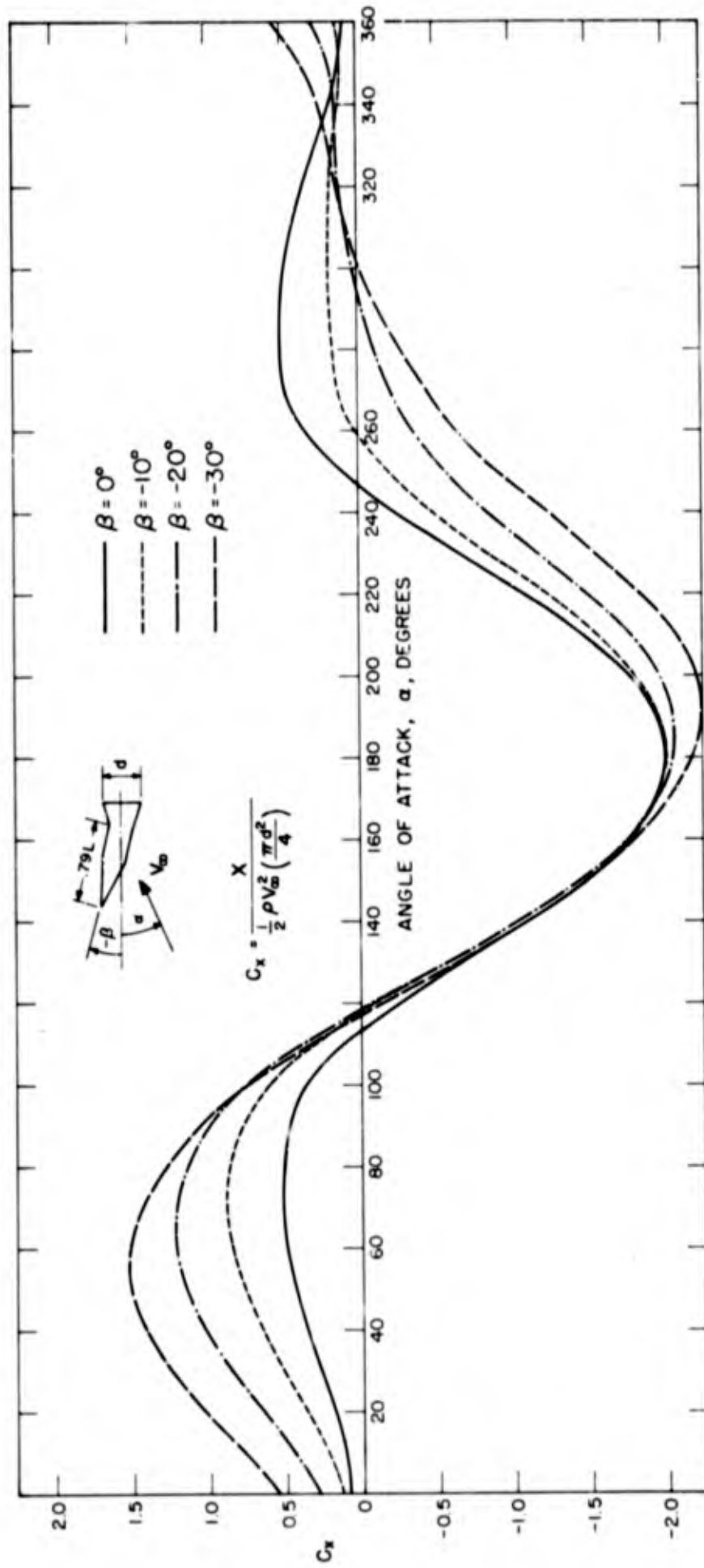
FIG. 15 AXIAL FORCE COEFFICIENT $C_x \sim$ CONE – CYLINDER – FLARE

$$C_x = \frac{X}{\frac{1}{2}\rho V_\infty^2 \left(\frac{\pi d^2}{4}\right)}$$

$\beta = 0°$
$\beta = -10°$
$\beta = -20°$
$\beta = -30°$

ANGLE OF ATTACK, α, DEGREES

50
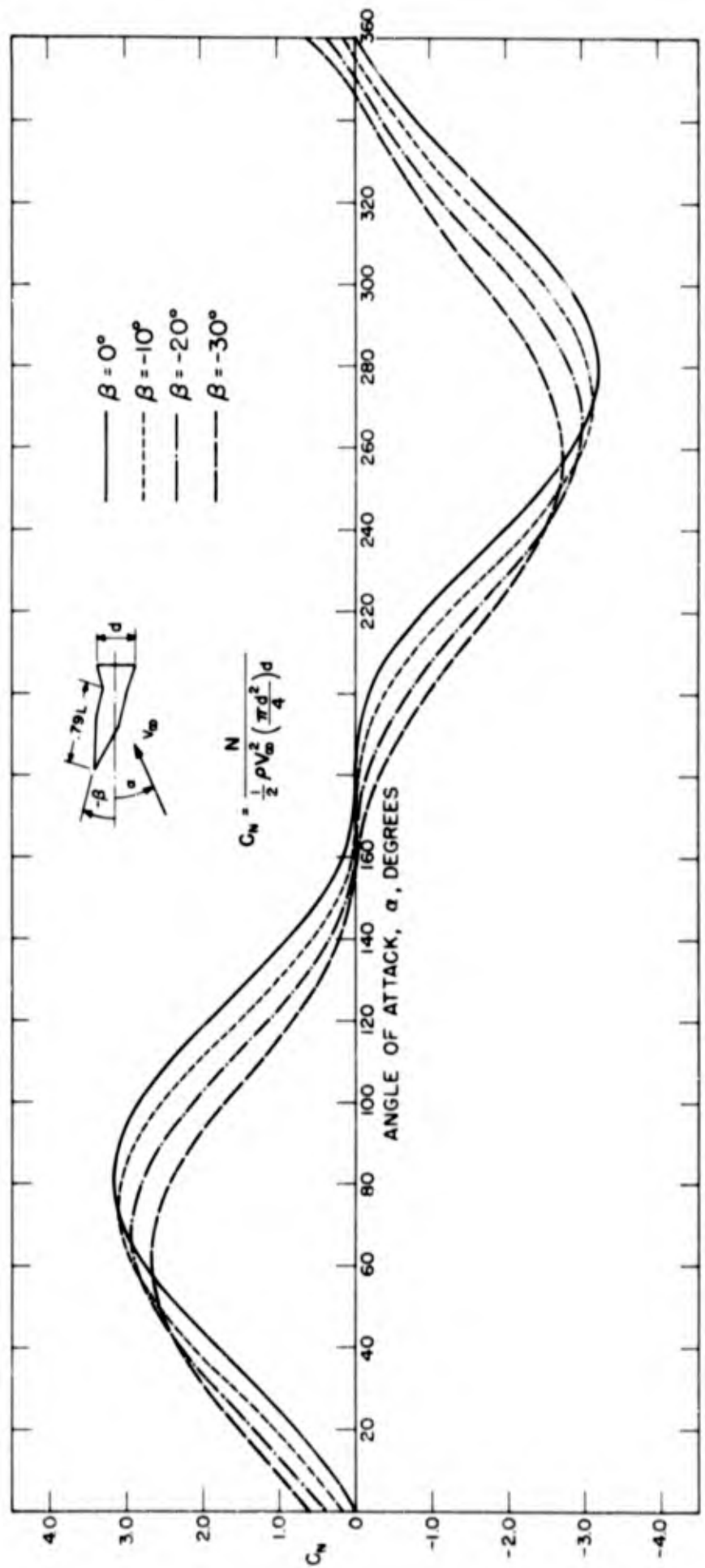
FIG. 16 NORMAL FORCE COEFFICIENT $C_N \sim$ CONE - CYLINDER - FLARE

$$C_N = \frac{N}{\frac{1}{2}\rho V_\infty^2 \left(\frac{\pi d^2}{4}\right) d}$$

51
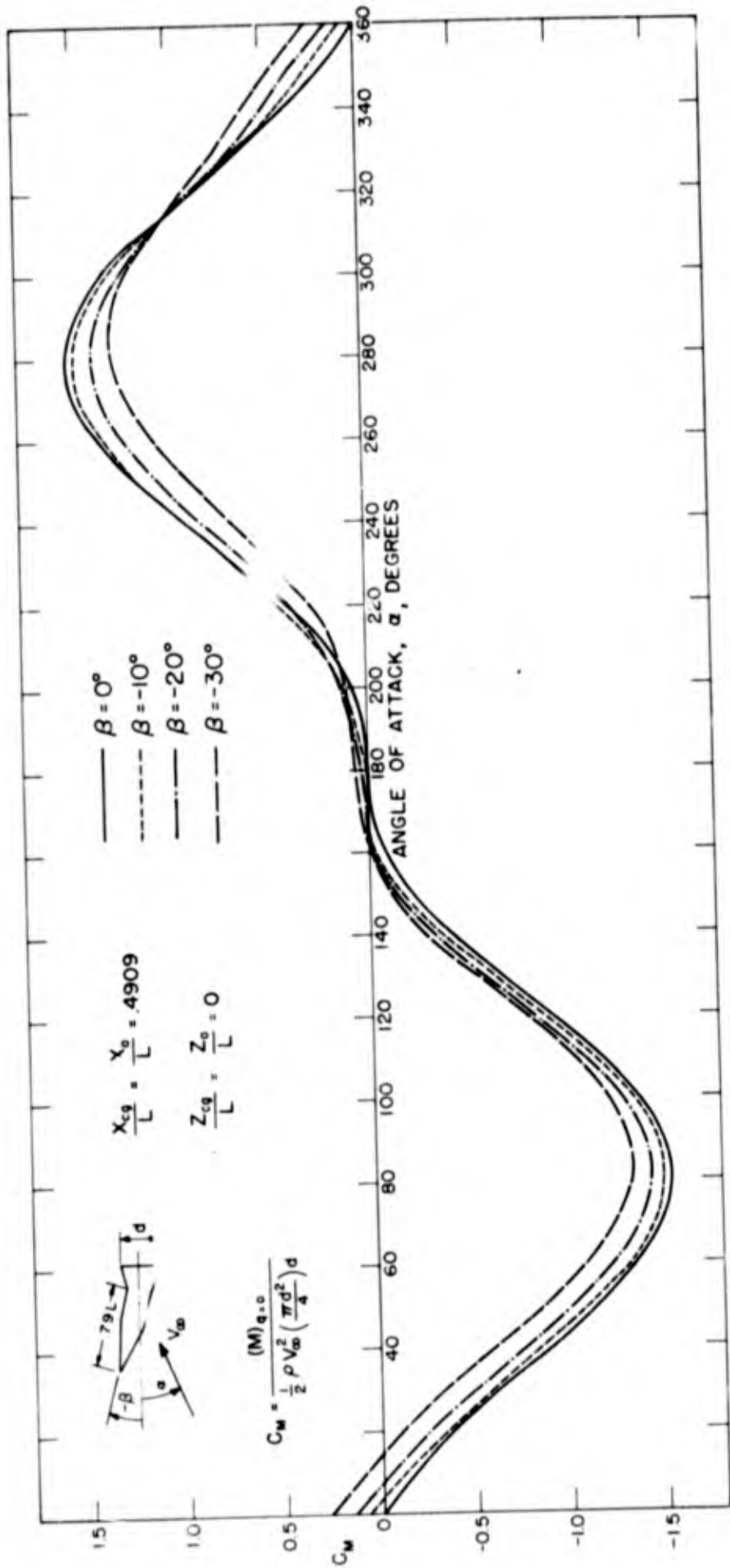
FIG. 17 STATIC PITCHING MOMENT COEFFICIENT C_M ~ CONE-CYLINDER-FLARE

$\beta = 0°$
$\beta = -10°$
$\beta = -20°$
$\beta = -30°$

$\dfrac{X_{cg}}{L} = \dfrac{Y_o}{L} = .4909$

$\dfrac{Z_{cg}}{L} = \dfrac{Z_o}{L} = 0$

$C_M = \dfrac{(M)_{q=0}}{\frac{1}{2}\rho V_\infty^2 \left(\frac{\pi d^2}{4}\right) d}$

ANGLE OF ATTACK, α, DEGREES
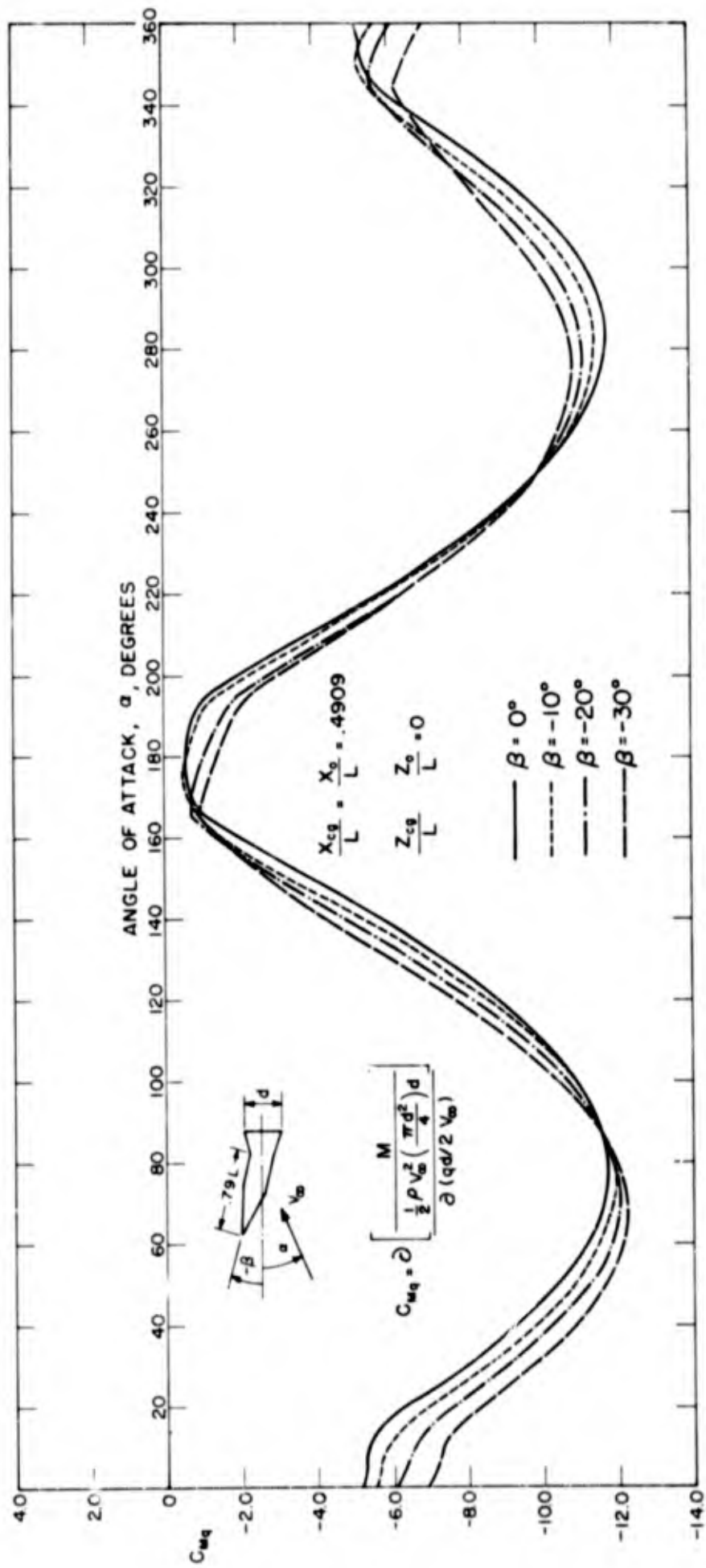
FIG. 18 PITCH DAMPING COEFFICIENT $C_{Mq} \sim$ CONE - CYINDER - FLARE
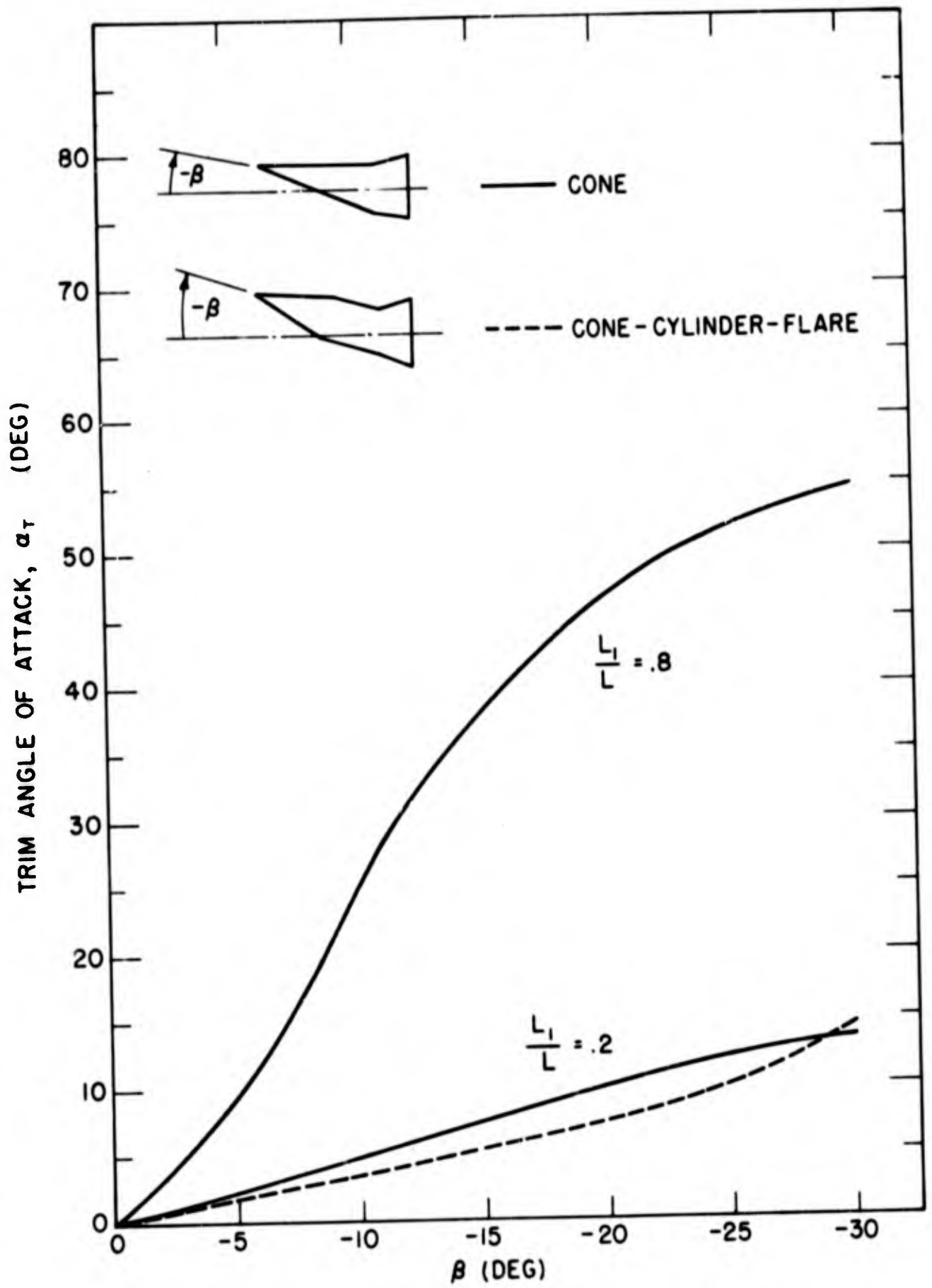
FIG. 19   EFFECT OF β ON TRIM ANGLE OF ATTACK

54

FIG. 20 EFFECT OF β ON L/D AT TRIM

.55
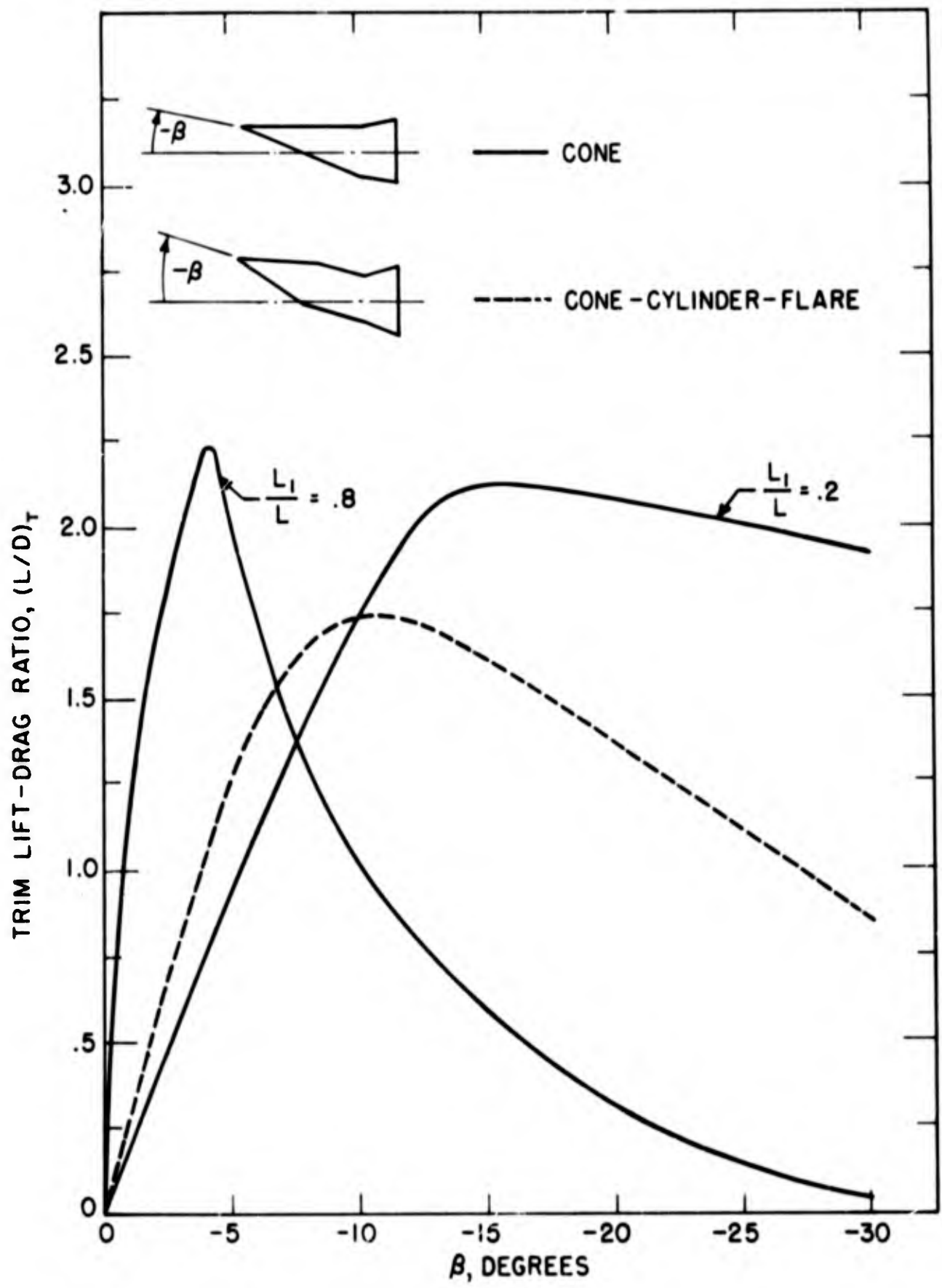
APPENDIX A

COMPUTER PROGRAM

A FORTRAN program for the IBM 1620 computer is presented which calculates the force and moment coefficients for combinations of bodies derivable from a right circular cone frustum. This program utilizes the theory presented in this report and calculates the coefficients for $0^o \le \alpha \le 360^o$. A complete program listing is given on page 71.

A.1 List of FORTRAN Symbols

FORTRAN Symbols	Mathemathical Symbols
A(I), B(I), C(I), ... I(I)	A_n, B_n, C_n, ... I_n
AANG	α_n
ALP(I)	α (in rad.)
ALPHA(I)	α (in deg.)
BETA(I)	β_n
CM	$C_M^{(n)}$
CMT	$C_{M_{tot}}$
CMQ	$C_{Mq}^{(n)}$
CMQT	$C_{M_{qtot}}$
CN	$C_N^{(n)}$
CNR	$C_{N_R}^{(n)}$
CNT	$C_{N_{tot}}$
CX	$C_X^{(n)}$
CXR	$C_{X_R}^{(n)}$
CXT	$(C_X)_{tot}$
DA	$\Delta\alpha$(in deg.)
DELTA(I)	δ_n
D'(I)	d_n/L

DOL	d/L
EL(I)	L_n/L
IBS(I)	types of nth segment
NA	no. of α's
NBS	no. of segments
PHONE	$\Phi_1^{(h)}$
PHTWO	$\Phi_2^{(h)}$
PHTHR	$\Phi_3^{(h)}$
PHFOR	$\Phi_4^{(h)}$
THONE	θ_1
THTWO	θ_2
XCGL	X_{cg}/L
XT(I)	$(X_T)_n/L$
XZL	x_0/L
ZCGL	z_{cg}/L
ZT(I)	$(z_T)_n/L$
ZZL	z_0/L

A.2 Flow Chart

A flow chart of the program is given in Figure A.1. The general steps in the calculations are outlined below. If more detail is desired, the program listing may be consulted.

1. The program first must read a series of control quantities which determine the number of cases to be computed and the range of α for which data will be obtained. These quantities appear on input cards 1 and 2 and their meanings are given in Section A.3 - Input Data.

2. Next, the program reads the nondimensional properties which are characteristic of the vehicle. These include the reference area, S/L^2, the length used for the moment coefficients, d/L, the point about which the moment is to be computed (x_o/L , z_o/L) and the C.G. position (x_{cg}/L , z_{cg}/L). (See Section A.3, card No.3).

3. The program enters a loop which reads and calculates data for each of the n segments. The input data describes the shape of the nth segment, and its orientation with respect to the principal axis system. (See Section A.3, card No. 4). The segments which are possible are a frustum, cone, cylinder, and circular base.

   If the segment is a frustum, cone, or cylinder, the x-integrations A_n, B_n, C_n, ... I_n are also evaluated for that segment, Eq. 3.2. The point about which the moment is to be computed and the C.G. position are expressed in the coordinate system of the nth segment, Eq. 4.4. After this calculation, the program

returns to read data (card No. 4) for another segment.

4. After completing the first loop, another large loop is
    entered. This loop starts with the given initial
    angle of attack and then increments through the range
    of angle of attack for which data is desired.

    Using the angle of attack, and hence the relative angle
    of attack, the forces and moment on each segment can
    be calculated once the amount of shielding is determined.
    The shielding depends on the type of body segment as
    well as the relative angle of attack.

5. If the nth segment is a rearward facing circular plate,
    the shielding criterion is simple. When the relative
    angle of attack is in the range $90^{o} \angle \alpha_n \angle 270^{o}$,
    the forces and moments on the plate are given by Eq.
    3.20. Otherwise, there is no contribution.

6. If the segment is a frustum, cone, or cylinder the
    shielding angles θ_1 and θ_2, are determined by the tests
    given in Eq. 2.41. The θ-integrations, $\Phi_1^{(h)}$, $\Phi_2^{(h)}$, $\Phi_3^{(h)}$,
    $\Phi_4^{(h)}$, Eq. 2.37, can then be found and used to calculate
    the force and moment due to that segment, Eqs. 2.32 -
    2.35.

7. When the nth segment is rotated, the normal and axial
    force on it must be resolved back to the principal
    axis system. This is done so that the forces on all
    segments will be in the same direction when they are
    summed. If the sense switch number 2 is off, the
    coefficients for each segment are punched. The program
    returns to STEP 4 for another segment.

8. The segment coefficients are added to obtain the total forces and moment on the composite body. These total body coefficients are then punched.

9. As an option, (sense switch No. 1), the total body coefficients may also be obtained as lift and drag coefficients, Eq. 4.7.

10. The program returns to STEP 4 and repeats STEPS 4 thru 10 for another angle of attack.
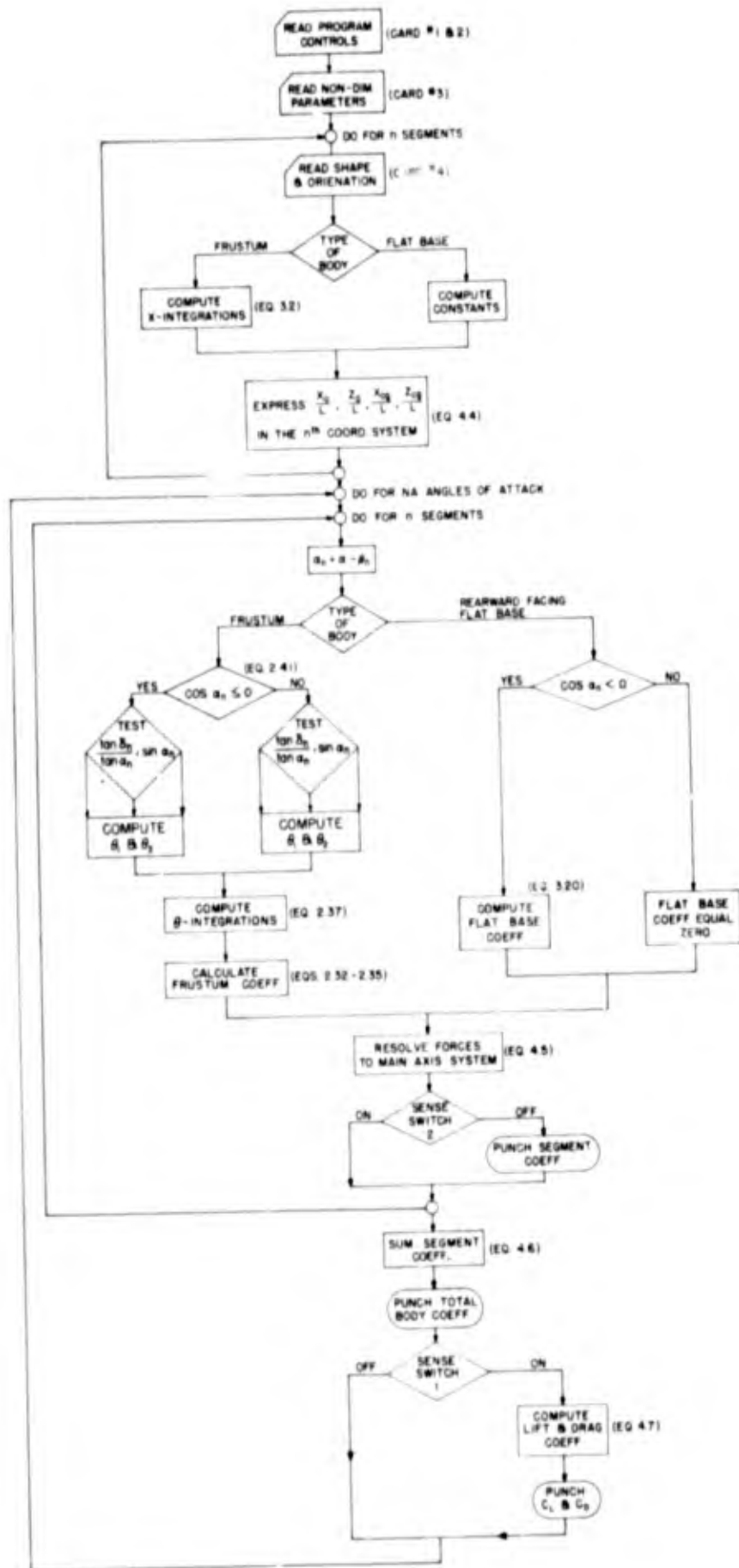
FIG. A.1 MAIN PROGRAM FLOW CHART

62

A.3 Input Information

Program Controls

II   A counter which controls the number of times which
            the angle of attack range and increment are to
            be changed. Set II = 1 if no change is desired.

IJ   A counter which controls the number of cases to be
            run for an angle of attack range. For example, it
            may be desirable to obtain within the same run, the
            coefficients for several composite body shapes, or
            to vary the center of gravity location for a given
            composite body shape.

NA   The total number of angles of attack. This number
            should include the initial angle of attack, also.

DA   The increment in angle of attack (in degrees).
ALP(1)   The initial angle of attack (in degrees). The
            program calculates coefficients starting with
            ALP(1), then increments by DA and re-calculates,
            until a total of NA calculations have been performed.

Vehicle Parameters

NBS   The number of body segments

TITLE(I)   Alphabetic information for a title for each case
            (limited to 24 characters, including spaces).

SLS   Nondimensional reference area, S/L^2.

DOL   Nondimensional reference diameter, d/L.

63

XZL	Nondimensional x-coordinate of the point about which the moment is to be computed, x_o/L.
ZZL	Nondimensional z-coordinate of the point about which the moment is to be computed, z_o/L.
XCGL	Nondimensional x-coordinate of the total body center of gravity, x_{cg}/L.
ZCGL	Nondimensional z-coordinate of the total body center of gravity, z_{cg}/L.

Segment Parameters

DELTA(I)	The frustum or cone half angle for the Ith segment (in degrees). Set DELTA(I) = 0.0 for a cylinder or a flat base.
BETA(I)	The rotation angle of the Ith segment (in degrees).
EL(I)	Nondimensional length of the Ith segment, L_n/L.
D(I)	Nondimensional front base diameter of the Ith segment d_n/L. For a cone segment, set D(I) = 0.0.
XT(I)	Nondimensional x-coordinate of the origin of the Ith segment,
ZT(I)	Nondimensional z-coordinate of the origin of the Ith segment,
IBS(I)	The class of body shape to which the Ith segment belongs.

IBS(I) = +1 means the segment is a frustum cone
or cylinder.

IBS(I) = +2 applies to a general body. This was
used to allow for later expansion of the program.
Do not use IBS(I) = +2.

IBS(I) = +3 means the segment is a flat base.

Input Format

Card No. 1
II	IJ	NA	DA	ALP(1)
I2	I2	I3	F7.2	F7.2

This card may be repeated II times. The last
card No. 1 should have II = +1

Card No. 2
NBS	TITLE(I)
I3	6A4

A card No. 2, card No. 3, and NBS number of card
No. 4 are required for each of the IJ cases.

Card No. 3
SLS	DOL	XZL	ZZL	XCGL
E13.8	E13.8	E13.8	E13.8	E13.8
ZCGL				
E13.8				

Card No. 4
DELTA(I)	BETA(I)	EL(I)	D(I)	XT(I)
F6.2	F6.2	E13.8	E13.8	E13.8
ZT(I)	IBS(I)			
E13.8	I3			

There are NBS number of card No. 4's required for
each card No. 2.

As an example, the following data apply for one of the
cases considered in Section V; a 10° cone broken upward at 0.8 of
its length.
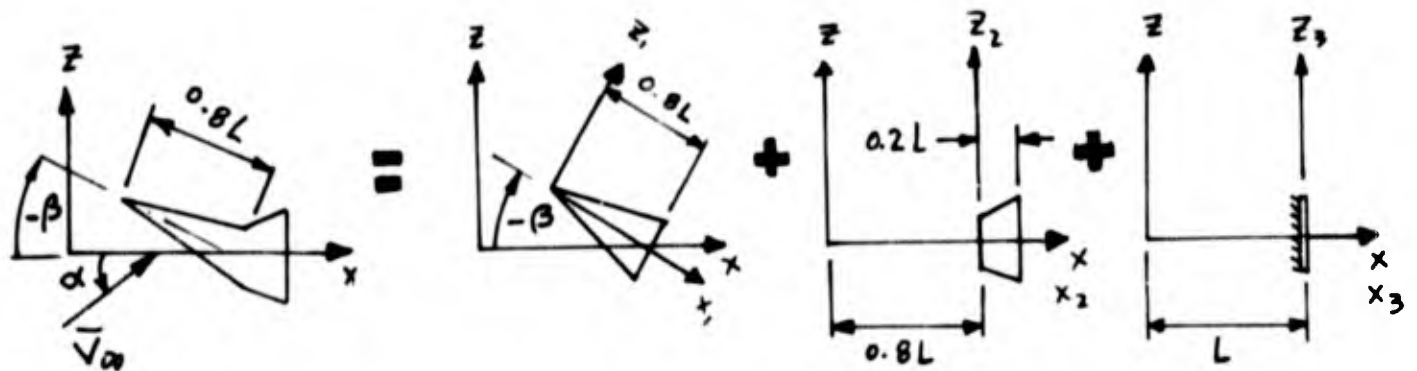
Card No. 1

II	IJ	NA	DA	ALP(1)
+1	+1	+73	5.0	0.0

Only one range of angle of attack will be used. Data will be calculated for $\alpha = 0°$ to $360°$ at $5°$ intervals. Only one configuration or case is considered.

Card No. 2

NBS	TITLE(I)
3	BENT CONE

— Card No. 3

SLS	DOL	XZL	ZZL	XCGL
0.0976792	0.35266	0.65	0.0	0.65

ZCGL
0.0

For this case, it was decided to nondimensionalize with respect to the base area, base diameter and total body length

Then

$$\frac{S}{L^2} = \frac{\pi d^2/4}{L^2} = \pi \tan^2 \delta$$

$$\frac{d}{L} = 2 \tan \delta$$

66

For the first segment (Cone):

Card No. 4

	DELTA(I)	BETA(I)	EL(I)	D(I)	XT(I)
	10.0	-6.0	0.8	0.0	0.00438248

	ZT(I)	IBS(I)
	0.0836228	+1

For the particular case of a bent cone, $(x_T)_1$ and $(z_T)_1$ are given by the equations

$$\frac{(x_T)_1}{L} = \frac{L_1}{L}\left(1 - \cos\beta_1\right)$$

$$\frac{(z_T)_1}{L} = -\frac{L_1}{L}\sin\beta_1$$

For the second segment (Frustum):

Card No. 4

	DELTA(I)	BETA(I)	EL(I)	D(I)	XT(I)
	10.0	0.0	0.2	0.282128	0.8

	ZT(I)	IBS(I)
	0.0	+1

For the third segment (Circular base):

Card No. 4

	DELTA(I)	BETA(I)	EL(I)	D(I)	XT(I)
	0.0	0.0	0.0	0.35266	1.0

	ZT(I)	IBS(I)
	0.0	+3

The output for this example is given on page 70 for $0 \leq \dot{\alpha} \leq 1\dot{5}$.

67

A.4 Output Information

Sense Switches

Sense Switch 1:

ON - The total body force coefficients will also be expressed as lift and drag coefficients, C_L and C_D.

OFF - No lift and drag coefficients.

Sense Switch 2:

ON - The force and moment contribution of each segment is **NOT** punched.

OFF - The coefficients for each segment are punched.

Output Key

Line 1:   Alphabetic information giving title.

Line 2:   S/L*L   nondimensional reference area, S/L^2

D/L   nondimensional diameter, d/L

XO/L   nondimensional coordinates of point about
ZO/L   which moment is computed, x_o/L, z_o/L

XCG/L   nondimensional coordinates of total body
ZCG/L   center of gravity, x_{cg}/L, z_{cg}/L.

Line 3:   A list of data pertaining to each of the segments. Data for each segment is given on a separate line.

L(N)/L   nondimensional segment length, L_n/L

DELTA   segment half angle (in degrees)

D(N)/L   nondimensional segment diameter, d_n/L

BETA   segment rotation angle (in degrees), β_n

X(T)/L   nondimensional coordinates of front of
Z(T)/L   segment, $(x_T)_n/L$, $(z_T)_n/L$

68

Line 4:   ALPHA   angle of attack (in degrees)
              SHAPE   the number of the segments
              CN   normal force coefficient, C_N

              CX   axial force coefficient, C_X

              CM   static moment coefficient, C_M

              CMQ   pitch damping coefficient, C'_{Mq}

              CL   composite body lift coefficient, C_L

              CD   composite body drag coefficient, C_D

If sense switch 3 is off, the segment coefficients are punched
as well as the total composite body coefficients. The segments
are numbered by the order in which the data is read.

The output for the example considered in Appendix A.3
follows.

BENT CONE

S/L•L = .09767 D/L = .35266 XO/L = .65000 ZO/L = 0.00000 XCG/L = .65000 ZCG/L = 0.00000

L(N)/L	DELTA	D(N)/L	BETA	X(T)/L	Z(T)/L
.80000	10.00	0.00000	-6.00	.00438	.08362
.20000	10.00	.28212	0.00	.80000	0.00000
0.00000	0.00	.35266	0.00	1.00000	0.00000

ALPHA	SHAPE	CN	CX	CM	CMQ	CL	CD
0.00							
	1	1.23640E-01	5.81981E-02	3.89227E-02	-9.59518E-01		
	2	0.00000E-99	2.17102E-02	0.00000E-99	-9.60201E-01		
	3	0.00000E-99	0.00000E-99	0.00000E-99	0.00000E-99		
	TOTAL	1.23640E-01	7.99084E-02	3.89227E-02	-1.91972E-00	1.23640E-01	7.99084E-02
5.00							
	1	2.25149E-01	8.37527E-02	6.92309E-02	-9.69460E-01		
	2	6.06271E-02	2.41974E-02	-4.84455E-02	-9.56548E-01		
	3	0.00000E-99	0.00000E-99	0.00000E-99	0.00000E-99		
	TOTAL	2.85777E-01	1.07950E-01	2.07853E-02	-1.92600E-00	2.75281E-01	1.32446E-01
10.00							
	1	3.29925E-01	1.15827E-01	1.00936E-01	-1.12364E-00		
	2	1.19412E-01	3.15834E-02	-9.54191E-02	-9.45614E-01		
	3	0.00000E-99	0.00000E-99	0.00000E-99	0.00000E-99		
	TOTAL	4.49337E-01	1.47410E-01	5.51749E-03	-2.06925E-00	4.16913E-01	2.23197E-01
15.00							
	1	4.45671E-01	1.52373E-01	1.36044E-01	-1.29621E-00		
	2	1.78759E-01	4.28661E-02	-1.42842E-01	-1.07742E-00		
	3	0.00000E-99	0.00000E-99	0.00000E-99	0.00000E-99		
	TOTAL	6.24431E-01	1.95239E-01	-6.79776E-03	-2.37364E-00	5.52622E-01	3.50201E-01

70

A.5 FORTRAN Program Listing

The program includes the following:

1. MAIN -   the main program which calculates the aero-
            dynamic coefficients for bodies composed
            of cone frusta and flat plates.

2. FRUST -   a subroutine to calculate the x-integra-
            tions, A_n, B_n, C_n, ... I_n for a typical
            conical frustum segment.

3. GENER -   a subroutine to allow for future program
            expansion. At the present time, no calcula-
            tions are performed by this subroutine.

4. ASINF -   a function which calculates the arcsine.
            Values from $-\frac{\pi}{2}$ to $+\frac{\pi}{2}$ are possible.

1.   MAIN

         DIMENSION ALPHA(100),ALP(100),TITLE(6),DELTA(6),BETA(6),EL(6),
        1DL(6),XT(6),ZT(6),IBS(6),COB(6),SIB(6),XOR(6),ZOR(6),XCGR(6),
        2ZCGR(6),A(6),B(6),C(6),D(6),E(6),F(6),G(6),H(6),EI(6),FP(6)
         COMMON A,B,C,D,E,F,G,H,EI,DELTA,EL,DL
```
1        READ 2,II,IJ,NA,DA,ALP(1)
2          FORMAT(2I2,I3,2F7.2)
         ALPHA(1)=.17453292E-1*ALP(1)
         DO 3 J = 2,NA
         ALP(J)=ALP(J-1)+DA
         ALPHA(J)=.17453292E-1*ALP(J)
3        CONTINUE
5        READ 4,NBS,(TITLE(I),I=1,6)
4        FORMAT(I3,6A4)
         READ 6,SLS,DOL,XZL,ZZL,XCGL,ZCGL
6        FORMAT(6E13.8)
         C1=2.0/SLS
         C4=4.0*C1/(DOL**2)
         PUNCH 7,(TITLE(I),I=1,6),SLS,DOL,XZL,ZZL,XCGL,ZCGL
7        FORMAT(1H1 6A4/ 8H0S/L*L =F8.5,7H  D/L =F8.5,8H  XO/L =F8.5,8H  Z
        10/L =F8.5,9H  XCG/L =F8.5/9H+ ZCG/L =F8.5//59H0 L(N)/L     DELTA
        2  D(N)/L     BETA      X(T)/L      Z(T)/L)
8        FORMAT(1H0,2(F8.5,3X,F6.2,3X),F8.5,3XF8.5)
         DO 15 I = 1,NBS
         READ 9,DELTA(I),BETA(I),EL(I),DL(I),XT(I),ZT(I),IBS(I)
9        FORMAT(2F6.2,4E13.8,I3)
         PUNCH 8,EL(I),DELTA(I),DL(I),BETA(I),XT(I),ZT(I)
         DELTA(I)=.17453292E-1*DELTA(I)
         BETA(I)=.17453292E-1*BETA(I)
         N=IBS(I)
         GO TO (10,11,12),N
10       CALL FRUST(I,FP(I))
         GO TO 13
11       CALL GENER(I,FP(I))
         GO TO 13
12       BCX=-1.5707963*(DL(I)**2)/SLS
         BCM=-BCX/DOL
         BCMQ=4.0*BCM/DOL
         BTRM=.0625*(DL(I)**2)
13       COB(I)=COSF(BETA(I))
         SIB(I)=SINF(BETA(I))
         DX=XZL-XT(I)
         DZ=ZZL-ZT(I)
         DXC=XCGL-XT(I)
         DZC=ZCGL-ZT(I)
         XOR(I)=DX*COB(I)+DZ*SIB(I)
         ZOR(I)=DZ*COB(I)-DX*SIB(I)
         XCGR(I)=DXC*COB(I)+DZC*SIB(I)
         ZCGR(I)=DZC*COB(I)-DXC*SIB(I)
15       CONTINUE
         PUNCH 16
16       FORMAT(75H0 ALPHA   SHAPE       CN          CX          CM
        1    CMQ          CL/9H+       CD)
         DO 40 J = 1,NA
         PUNCH 17,ALP(J)
17       FORMAT(1H0F7.2)
         CNT=0.0
         CXT=0.0
         CMT=0.0
```

```
      CMQT=0.0
      DO 35 I = 1,NBS
      AANG=ALPHA(J)-BETA(I)
      CO=COSF(AANG)
      S=SINF(AANG)
      IF(IBS(I)-3) 22,18,22
18    IF(CO) 19,20,20
19    CS=CO**2
      CN = 0.0
      CX=BCX*CS
      CM=BCM*CS*ZOR(I)
      CMQ=BCMQ*CO*(ZOR(I)*ZCGR(I)+BTRM)
      GO TO 330
20    CNR=0.0
      CXR=0.0
      CM=0.0
      CMQ=0.0
      GO TO 33
22    IF(ABSF(CO)-.000001) 25,25,23
23    IF(ABSF(S/CO)-ABSF(FP(I))-.000000001) 24,24,25
24    IF(FP(I)*CO) 20,20,28
25    ARG=FP(I)*CO/S
      THET=ASINF(ARG)
      IF(S) 27,26,26
26    THONE=-1.5707963
      THTWO=THET
      GO TO 31
27    THONE=THET
      THTWO=1.5707963
      GO TO 31
28    THTWO=1.5707963
      THONE=-THTWO
31    PHONE=2.0*(THTWO-THONE)
      IF(ABSF(PHONE)-.00001) 20,20,32
32    CUNO=COSF(THONE)
      CDOS=COSF(THTWO)
      PHTWO=2.0*(CUNO-CDOS)
      PHTHR=0.5*(PHONE+SINF(2.0*THONE)-SINF(2.0*THTWO))
      PHFOR=PHTWO+.66666667*(CDOS**3-CUNO**3)
      CP1=CO*PHONE
      CP2=CO*PHTWO
      CP3=CO*PHTHR
      SP2=S*PHTWO
      SP3=S*PHTHR
      SP4=S*PHFOR
      ACBS=A(I)*CP1-B(I)*SP2
      CSBC=C(I)*SP3-B(I)*CP2
      CCDS=C(I)*CP3-D(I)*SP4
      ECFS=E(I)*CP2-F(I)*SP3
      GSFC=G(I)*SP4-F(I)*CP3
      CX=C1*(CO*ACBS+S*CSBC)
      CN=C1*(CO*CSBC+S*CCDS)
      CM=(C1*(CO*ECFS+S*GSFC)+XOR(I)*CN-ZOR(I)*CX)/DOL
      CMQ=C4*(CSBC*(ZOR(I)*XCGR(I)+XOR(I)*ZCGR(I))-XOR(I)*XCGR(I)*CCDS
     1 -ZOR(I)*ZCGR(I)*ACBS+EI(I)*SP4-H(I)*CP3+ECFS*(ZOR(I)+ZCGR(I))-
     2 GSFC*(XCGR(I)+XOR(I)))
330   CXR=CX*COB(I)-CN*SIB(I)
      CNR=CX*SIB(I)+CN*COB(I)
      CNT=CNT+CNR
      CXT=CXT+CXR
```

```
        CMT=CMT+CM
        CMQT=CMQT+CMQ
3       IF(SENSE SWITCH 2) 35,39
39      PUNCH 34,1,CNR,CXR,CM,CMQ
34      FORMAT(1H 10X,I2,1X,4(1X,E12.5))
35      CONTINUE
        IF(SENSE SWITCH 1) 37,38
37      CA=COSF(ALPHA(J))
        SA=SINF(ALPHA(J))
        CD=CNT*SA+CXT*CA
        CL=CNT*CA-CXT*SA
        PUNCH 36,CNT,CXT,CMT,CMQT,CL,CD
        GO TO 40
38      PUNCH 36,CNT,CXT,CMT,CMQT
40      CONTINUE
36      FORMAT(1H0,8X,5HTOTAL,5(1X,E12.5)/1H+E12.5)
        IJ = IJ - 1
        IF(IJ) 42,42,5
42      II = II - 1
        IF(II) 43,43,1
43      CALL EXIT
        END
```

```
2.    SUBROUTINE FRUST(I,TD)
      DIMENSION A(6),B(6),C(6),D(6),E(6),F(6),G(6),H(6),EI(6),DELTA(6),
     1EL(6),DL(6)
      COMMON A,B,C,D,E,F,G,H,EI,DELTA,EL,DL
      CO=COSF(DELTA(I))
      S=SINF(DELTA(I))
      TD=S/CO
      SS=1.0/(CO**2)
      Q=EL(I)*TD
      CON=EL(I)*(DL(I)+Q)
      SL=(EL(I)**2)*SS
      CTO=0.5*DL(I)*TD*CON+SL*(0.5*DL(I)+.66666667*Q)
      CTH=SL*SS*(CON-0.5*EL(I)*Q)+DL(I)*(SL*(.75*TD*DL(I)-.66666667*EL
     1(I))+.25*DL(I)*Q*(DL(I)-EL(I))))
      R=0.5*CON*S
      B(I)=S*R
      C(I)=CO*R
      D(I)=0.5*CO*CO*CON
      A(I)=TD*B(I)
      T=0.5*CTO*CO
      G(I)=CO*T
      F(I)=S*T
      E(I)=S*F(I)/CO
      W=0.5*CO*CTH
      H(I)=S*W
      EI(I)=CO*W
      RETURN
      END
```

```
3.   SUBROUTINE GENER(I,FP)
     RETURN
     END
```

```
4.           FUNCTION ASINF(XX)
    C         RANGE -1 L.E. X L.E. +1,  -PI/2 L.E. ASIN L.E. +PI/2
    1         X=ABSF(XX)
              IF (X-1.0) 11,11,4
   11         PSI=(((((((-.0012624911*X+.0066700901)*X-.017088126)*X+.030891881)*
             1X-.050174305)*X+.088978987)*X-.214598880)*X+1.5707963
              ASINF=1.5707963-SQRTF(1.0-X)*PSI
              IF(XX) 2,3,3
    2         ASINF=-ASINF
    3         RETURN
    4         PRINT 100,XX
              CALL EXIT
  100         FORMAT (/34HARGUMENT IN ASINF GREATER THAN 1.0E18.8)
              END
```